

# **Systems analysis of modular HIF development paths**

**Grant Logan**

**Director**

**Heavy-Ion Fusion Virtual National Laboratory**

- **Technical approach and constraints for modular HIF development**
- **Comparing quads and solenoids for modular linac transport**
- **Issues and R&D needs**

**SYNOPSIS:** This talk on issues and opportunities for modular HIF linac systems builds upon my earlier work in 1996 on applications of laser-produced high charge state ion sources for solenoid-focused linacs [unpublished MathCAD report entitled: "Modular ion induction drivers for inertial fusion drivers", November 21, 1996, which was described in a seminar at LBNL that year], and on the work of Lee and Briggs ["The solenoid transport option: IFE drivers, near-term research facilities, and beam dynamics", LBNL-40774, UC-419, HIFAN 914, September 1997]. The motivation of both efforts was to seek a lower-cost development path for heavy-ion fusion. The HIFSA study during the 80's considered solenoid transport for the front end of drivers and also ions with higher charge states 3-4. Those features were estimated to save ~30% in driver costs in the HIFSA studies, but several concerns discouraged further consideration of these options: availability of adequate sources and injectors, emittance growth due to larger beam currents, and difficulty in focusing higher perveance beams in the target chamber. Advances in target designs allowing larger focal spots, plasma neutralization and assisted pinch work to focus higher perveance beams, multi-beamlet injectors, and accel-decel solenoid bunching, all motivate reconsideration of modular approaches to HIF, both quad and solenoid options, that require higher current beams of higher  $q/A$  ions. The present HIF-VNL experimental facilities (HCX, NTX, STS-500 and IBX) and computer codes can address most of the technical issues that must be faced for any modular HIF approach.

**The multi-beam quad-array linac concept was selected to meet expected focusing needs for small-spot targets, and to minimize emittance & cost.**

**Robust-Point Design optimizes 120-beam quad-focused driver: 7.0 MJ, 4 GeV Bi<sup>+1</sup>, 35,600 tons of induction cores, 1834 HLPs, \$2.8 B tot capital cost**

**1.6 MeV  
0.63 A/beam  
30  $\mu$ s  
120 beams**

**Multiple  
Ion  
Source/  
Injectors**

**Multiple-Beam Acceleration**

**Induction Cores 35,600 tons**

**3 km**

**Common**

**4 GeV Bi<sup>+1</sup>  
94 A/beam  
200 ns**

**Drift compression**

**400 m**

**Bending**

**Final  
focusing**

**Chamber  
transport**

**Target  
Input  
7 MJ  
Yield  
400 MJ**

**4 GeV  
1.9 kA/beam  
9.3 ns**

**Relative beam bunch length at end of:**

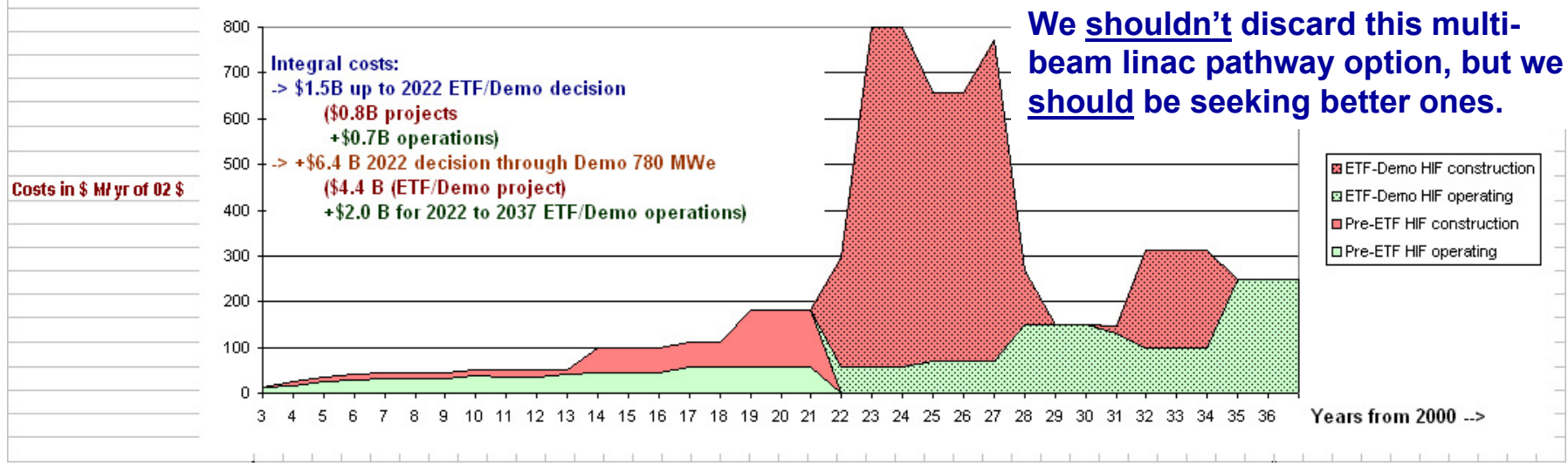
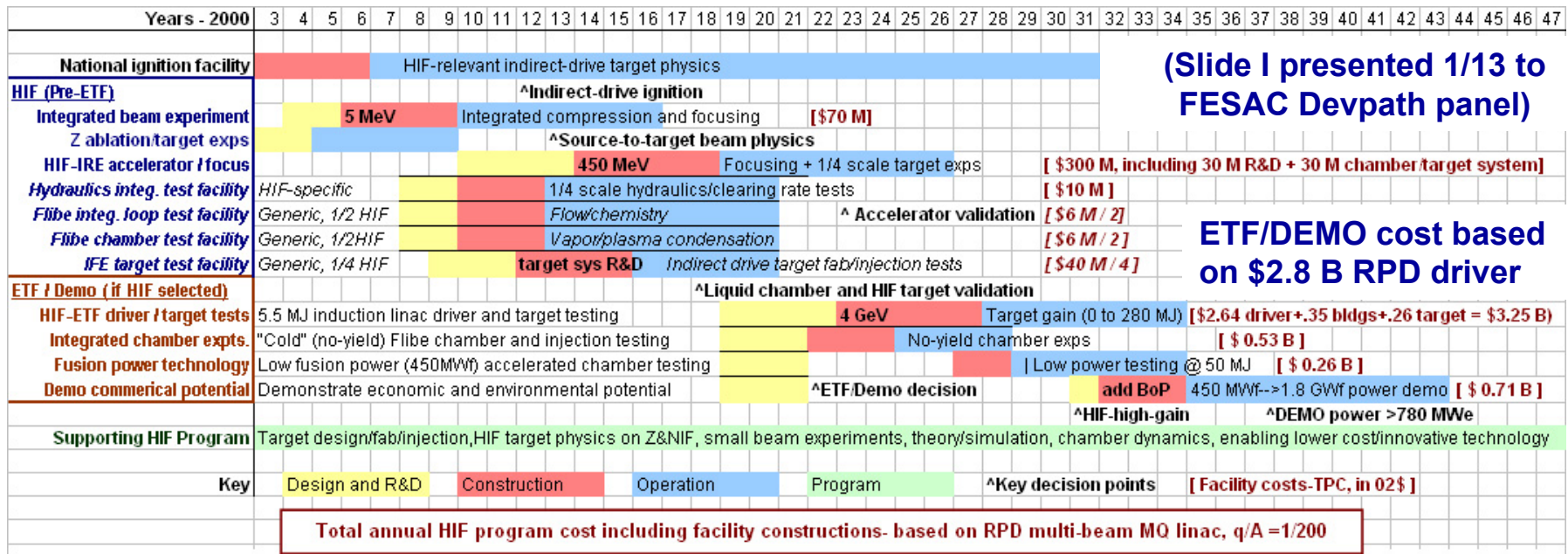
**injection**

**acceleration**

**drift compression**

***Multi-beam induction linac driver (RPD) cost increased recently to obtain consistency with detailed distributed-radiator target requirements for spot size, chamber emittance growth, symmetry, pulse shape, and illumination angles.***

# We need a faster, cheaper HIF development than the current pathway based on single multi-beam induction linacs, to meet fusion competition.



## We are developing new targets, to be tested on Z at SNL in FY04 with larger spot sizes that may allow drivers with as few as 16 to 32 beams

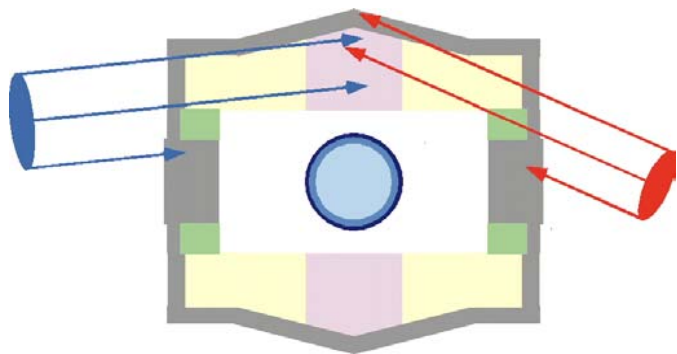


Fig. 2a: Distributed-Radiator Target (DRT) for 120 beams up to 24 degree incident angle. Allows 2 mm focal spot radii for 6 m focal length requiring plasma neutralization in the target chamber, with allowances for  $\epsilon_n < 0.9 \pi$  mm-mr normalized beam emittance and  $0.9 \times 10^{-3} \delta p/p$  momentum spread before final focus.

**→What lower-cost induction driver concepts might be enabled with improved focusing schemes and with 5 x larger allowed transverse and parallel beam emittances?**

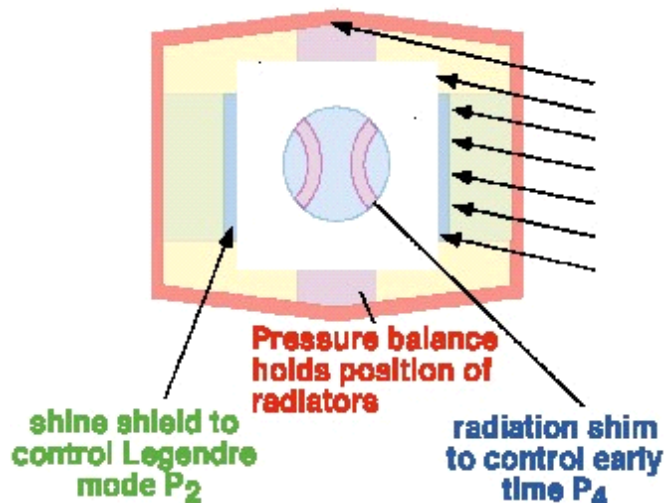


Fig. 2b: Hybrid Target (HT) allows larger 5 mm focal spot radii with fewer beam directions (16) at smaller incident angles (<10 degrees). Allows  $\epsilon_n > 5 \pi$  mm-mr normalized accelerator beam emittance at  $> 5 \times 10^{-3} \delta p/p$  momentum spread @ 6 m focal length.

**Besides the hybrid, Debbie Callahan is also considering other options for larger spots, simpler pulse-shaping, single ion energy**



# We are considering plasma neutralization throughout drift compression, cusp and/or assisted pinch focusing to accommodate the higher peak currents (100 kA) needed for fewer beams

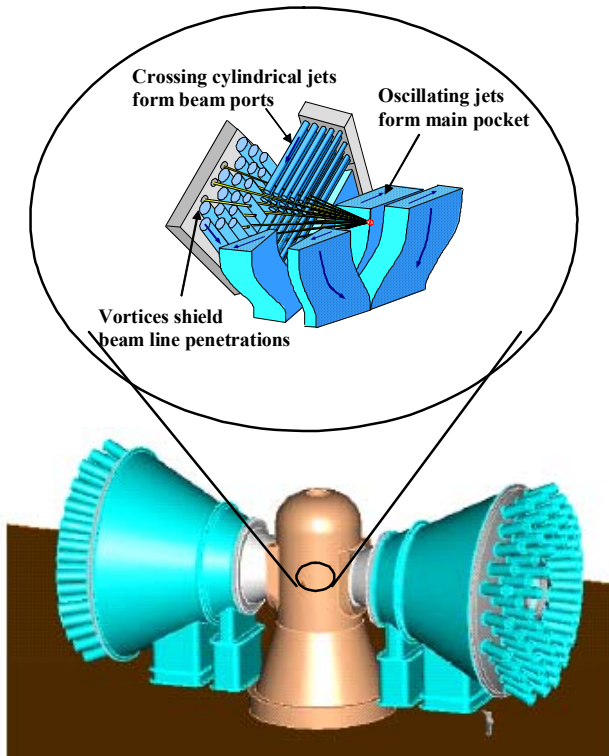


Fig.5a: The HYLIFE-II chamber concept uses fixed and oscillating jets of molten salt (inset) to protect the beam ports and chamber walls. Shown with 120-beam (60 each end) final focus magnet array for the DRT target (Fig.2a) consistent with the quadrupole linac driver (case in Fig.4a).

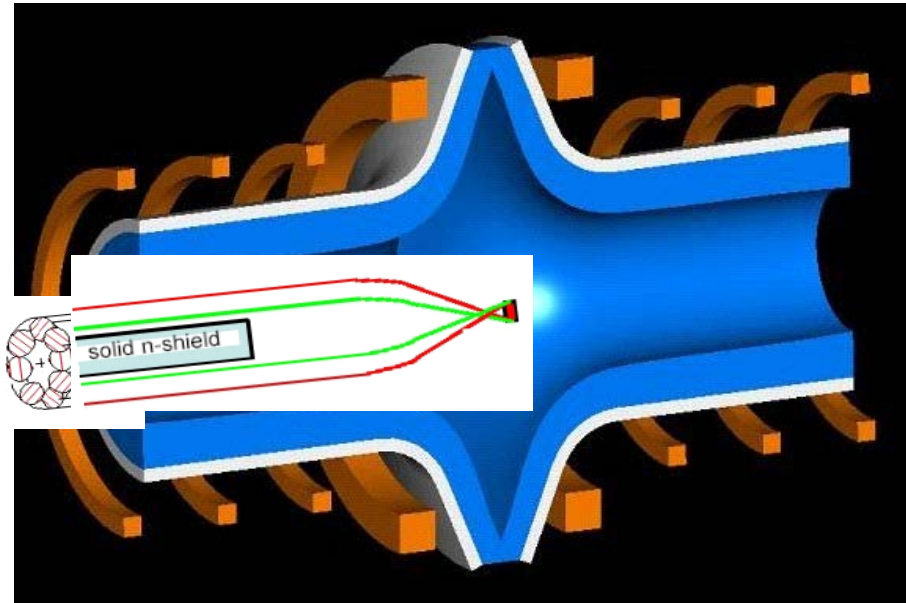


Fig.5b: Molten-salt vortex (blue) chamber concept integrated with a **magnetic cusp** that focuses an annulus of heavy-ion beams from a solenoid-linac driver (case in Fig.4b) to a HT hybrid target (Fig.2b) at the central field null in the chamber. One set of beams shown in a symmetric two-sided illumination. **Dense target debris plasma** ( $n_e > 10^{15}/\text{cm}^3$ ) leaks slowly from the central cusp filling the solenoid drift lines between shots, providing full plasma neutralization of beam space-charge throughout drift compression and the cusp-focus-chamber to the target. **Assisted pinch channels** can also be used.

# Along with enhanced forms of neutralized ballistic focusing, assisted pinch transport has become a second realistic focusing option for 100 kA-scale beams onto 5 mm radius-spot targets

PHYSICS OF PLASMAS

VOLUME 10, NUMBER 6

JUNE 2003

←June 2003

## Assisted-pinch transport of heavy-ion beams in a fusion chamber

D. R. Welch,<sup>a)</sup> T. C. Genoni, D. V. Rose, B. V. Oliver, and R. E. Clark  
*Mission Research Corporation, 5001 Indian School Road NE, Albuquerque, New Mexico 87110*

C. L. Olson  
*Sandia National Laboratories, P.O. Box 5800, Albuquerque, New Mexico 87185*

S. S. Yu  
*Lawrence Berkeley National Laboratory, 1 Cyclotron Road, Mail Stop 47-112, Berkeley, California 94720*

(Received 3 February 2003; accepted 5 March 2003)

In heavy-ion inertial confinement fusion, ion beams are transported several meters through the reactor chamber to the target. This standoff distance mitigates damage to the final focus magnets and chamber walls from the target explosion. A promising transport scheme makes use of a preformed discharge channel to confine and guide the beams. In this assisted-pinch transport scheme, many individual beams are merged into two high-current beams for two-sided illumination of the fusion target. The beams are combined and focused outside the chamber before propagating at small radius in the discharge channel to the target. A large beam divergence can be contained by the strong magnetic field resulting from the roughly 50-kA discharge current. Using a hybrid particle-in-cell simulation code, we examine the dynamics of heavy-ion inertial confinement fusion driver-scale beams in this transport mode. Results from detailed two-dimensional simulations of assisted-pinch transport in roughly 1-Torr Xe suggest that the Xe plasma becomes sufficiently conductive to limit self-field effects and achieve good transport efficiency. Coupling to a published target design is calculated. In addition, results from a semianalytic theory for resistive hose growth are presented that explain three-dimensional simulation results. © 2003 American Institute of Physics. [DOI: 10.1063/1.1570421]

**3 MJ/end @ < 5mm radius →  
6 MJ total into a hybrid target**

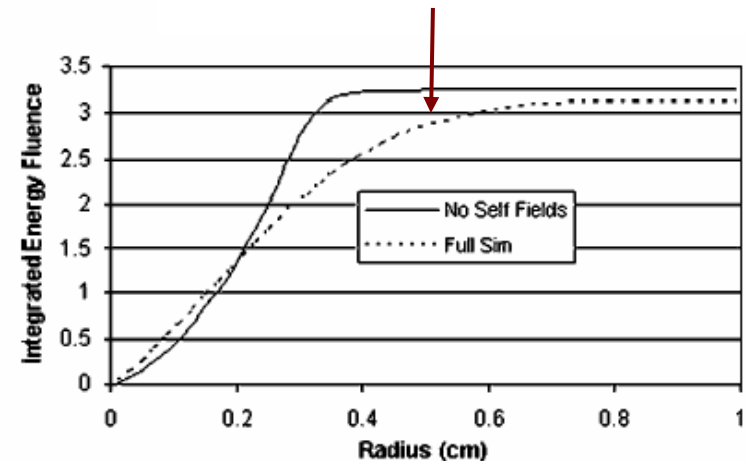


FIG. 4. The time-integrated beam energy deposition at the target ( $z = 450$  cm) is plotted for the nominal beam/channel simulations. The energy has been radially integrated to yield the beam energy contained within a given radius.

**Assisted pinch transport can help focus high current beams in compact final-focus, but must be married to a lower-cost linac to obtain any significant reductions in HIF driver cost and development.**

# **Could “modular” linac systems reduce HIF development cost and schedule, and still lead to a feasible, affordable driver?**

---

- A “modular” driver system means separated, identical induction linacs (modules), costing not more than the RPD for the same energy, and desirably much less.
- An IRE which provides full validation of one driver module.
- An IBX which provides proof-of-principle for the IRE/driver module.

## **Possible modular driver transport options to consider:**

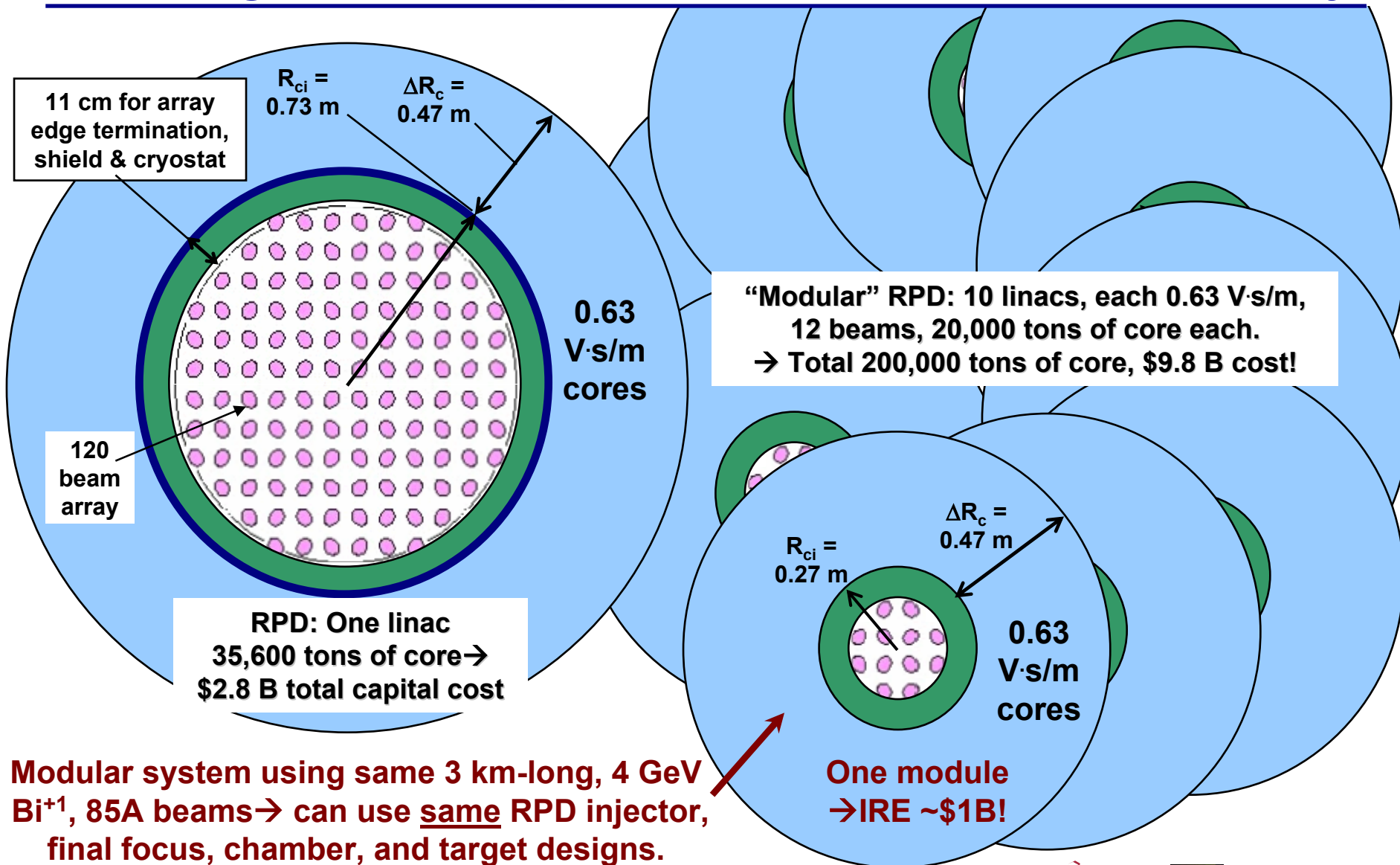
- 1. Single-beam solenoid linac modules**
- 2. Single-beam or few-multiple-beam quadrupole linac modules**
- 3. Single-beam hybrid-solenoid-quad linac modules**

## **Cost-competitive modular systems will likely require:**

- **$\ll 100$  linac modules @  $\ll 1$  GV and  $q/A \gg 0.01$**
- **Neutralized drift compression and final focus for higher currents/beam**
- **Larger target spot sizes  $> 2$  mm radius (e.g. hybrid targets).**

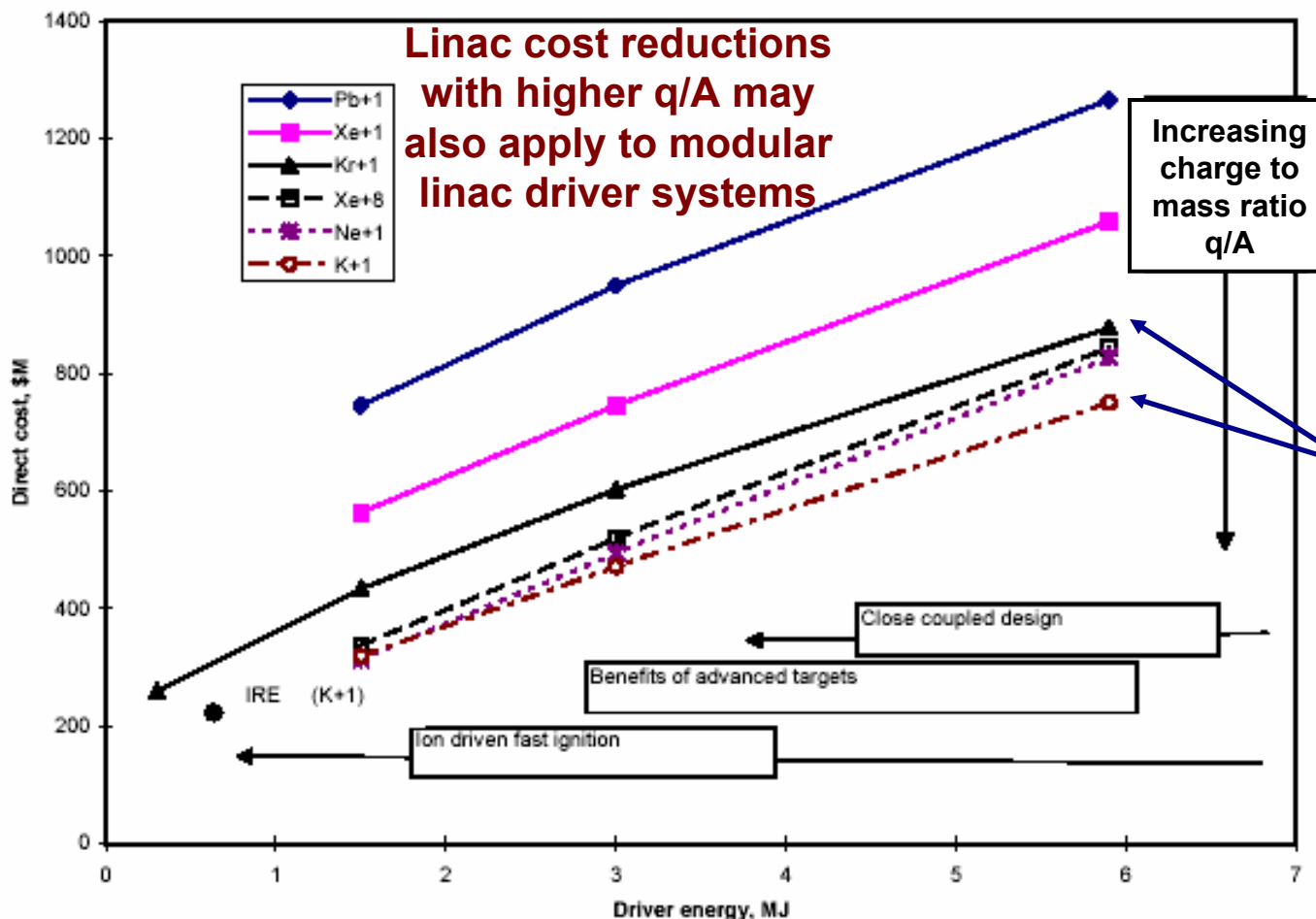


# The straightforward approach to modular HIF is too costly



# Increasing ion charge-to-mass-ratio for the same range reduces linac voltage, length and cost, provided injectors and final focus are improved to handle the associated higher beam currents

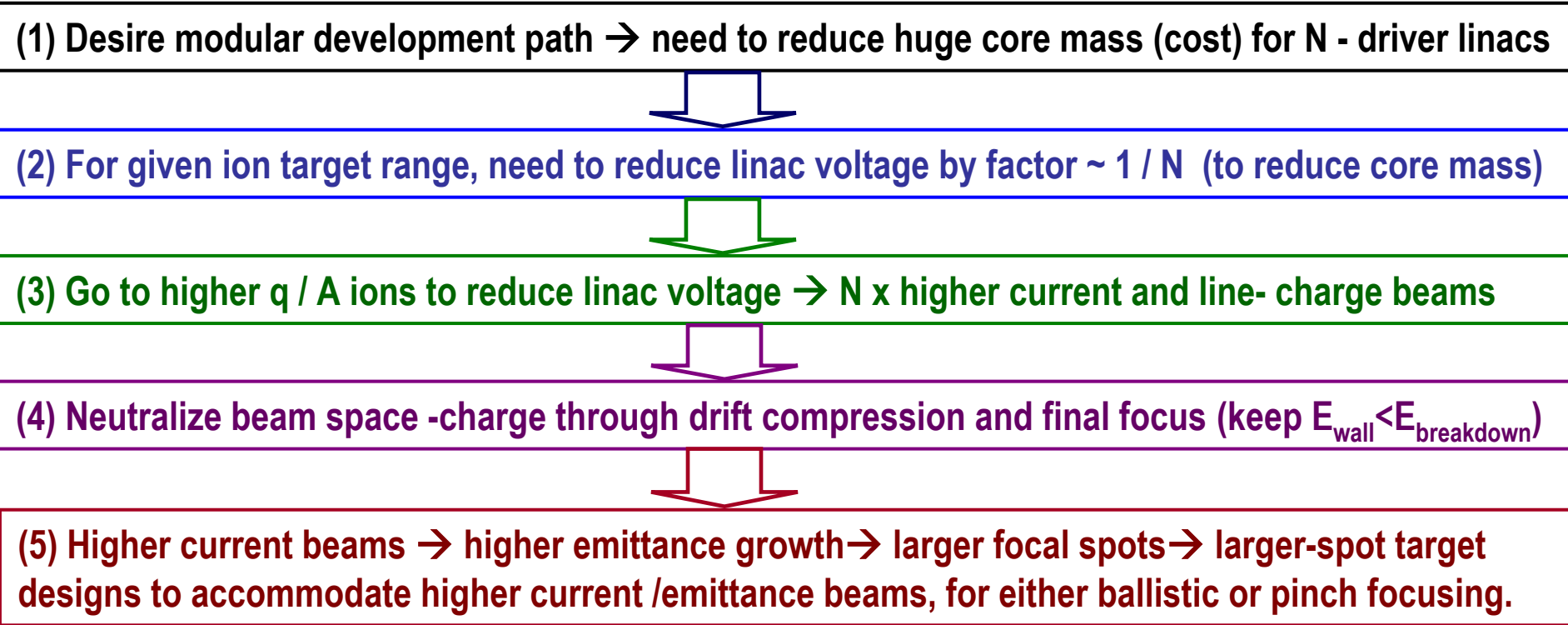
(Wayne Meier's 1997 systems analysis of multi-beam quad drivers using the IBEAM code. The HIFSA study also found similar cost savings comparing Cs+3 with Cs+1 ions.)



Increasing difficulties to meet target spots with neutralized ballistic focusing discouraged going to high  $q/A$

Increasing injector and "front-end" costs limit the potential cost savings at very high  $q/A$  for standard hot-plate-type injectors

# Guiding logic for modular induction linac development (quad or solenoid)



- Quadrupoles versus solenoids for transport: LINAC DESIGN ISSUES
- Injector current, size and cost versus allowed initial bunch compression rates in the front end
  - Average radial and longitudinal beam current density within cores (allowed average acceleration gradients at high  $q/A$ , radial and axial gaps needed for induction gradient and core flux-shielding).
  - Halo / beam loss, vacuum limits, and suppression of electron cloud effects

# ModSoLinac systems analysis finds 10 solenoid cases consistent with injection &focusing

Case No.	Ion charge state	Ion mass No.	Final ion K.E. (GeV)	Target energy (MJ)	Target spot size (mm)	Pulse @ target (ns)	No. of linacs, (=no. of beams)	No. of pulses per linac	Bunch charge (μC)	Linac MV & approx. length (m)	Allowed emittance growth	Est. core mass (10 <sup>3</sup> tons)
i =	qi =	Ai =	$\frac{Tf_i}{10^9}$	$\frac{Ed_i}{10^6}$	$\frac{rs_i}{10^{-3}}$	$\frac{\tau f_i}{10^{-9}}$	Nli =	Npi =	$\frac{Cb_i}{10^{-6}}$	$\frac{Lao_i}{10^{-6}}$	$\frac{\epsilon_{net_i}}{10^{-6}}$	$\frac{MFm_i}{10^3}$
1	8	131	2.5	6.7	5	9	16	2	670	313	11.6	6.9
2	26	131	2.5	6.7	5	9	46	2	757	96	9.6	6.1
3	1	40	0.5	4	4	28	18	2	222	500	7.4	12.5
4	8	131	2.5	4	4	28	10	2	640	313	9.3	4.3
5	26	131	2.5	4	4	28	27	2	770	96	7.8	3.6
6	1	20	0.2	6	8	28	25	3	400	200	18.8	6.9
7	1	40	0.5	6	8	28	18	3	222	500	28.7	12.5
8	8	40	0.5	6	8	28	52	3	615	63	20.8	4.5
9	8	131	2.5	6	8	28	9	3	711	313	34.4	3.9
10	26	131	2.5	6	8	28	27	3	770	96	32.6	3.6

Case No.	Injection energy (MeV)	Linac bunch comp. ratio	Injector pulse (μs)	Injector current (A)	Beamlet current density (mA/cm2)	Source array radius (m)	Injected bunch length (π mm-mr)	Injector emittance	Peak linac beam kA	Velocity tilt for drift (%)	Final tot. longit. spread(%)	Focus angle (mr)
i =	$\frac{qi \cdot V_o}{10^6}$	$\frac{bf_i}{10^{-6}}$	$\frac{\tau o_i}{10^{-6}}$	Io_i =	Jsi =	asi =	Lo_i =	$\frac{\epsilon sn_i}{10^{-6}}$	$\frac{Ia_i}{10^3}$	$\frac{\Delta ppc_i}{0.01}$	$\frac{\Delta ppt_i}{0.01}$	$\frac{\theta_i}{10^{-3}}$
1	24	8	8	83	157	0.34	48	6.8	6.7	B <sub>m</sub> 1.79	1.04	25
2	78	4	2.2	339	316	0.48	24	9.7	7.6	E <sub>m</sub> 1.79	0.98	25
3	3	16	20.5	11	95	0.16	78	5.7	2.2	B <sub>m</sub> 1.45	0.65	26
4	24	8	8	80	157	0.34	48	6.8	6.4	B <sub>m</sub> 1.79	0.66	26
5	78	8	4.5	173	297	0.35	48	7.1	7.7	E <sub>m</sub> 1.79	0.78	24
6	3	16	13	31	138	0.22	69	11.3	4	B <sub>m</sub> 2.17	1	31
7	3	16	20.5	11	95	0.16	78	5.7	2.2	B <sub>m</sub> 2.42	0.92	31
8	24	8	3.6	170	303	0.35	39	12.7	6.2	E <sub>m</sub> 2.42	1.02	32
9	24	16	16.1	44	150	0.24	95	4.9	7.1	B <sub>m</sub> 2.98	1.14	31
10	78	8	4.5	173	297	0.35	48	7.1	7.7	E <sub>m</sub> 2.98	1.11	32

Note: Target symmetry forces more beams than E or B limits only in case 4 (10 vs 9)      ^E or B limited

Table 13, p.38, ModSoLinac7. Cases meet all four of the following primary criteria: (1) minimum number of beams/linacs set by the greatest of target symmetry requirements, peak wall E-field limit in the transport channel, and solenoid field limit of 9 T for a common beam radius of 15 cm and pipe radius of 17 cm; (2) ballistic, plasma neutralized focusing to the target spot size at optimum focusing angles; (3) net allowed normalized emittance growth budget in the linac > 5 π mm-mr, *after* accounting for beamlet source array size, injector emittance and longitudinal momentum spread multiplied by the subsequent bunch compression ratios; and (4) a total estimated induction core mass less than half of the Snowmass baseline linac system. Common assumptions for all cases: ion range = 0.03 gm/cm2, 15% beamlet source array fill factor, extraction field = half of maximum transport electric field, source effective ion temperature = 2 eV, induction pulse length at end of linac τ<sub>a</sub> = 100 ns, macro-pulse durations for drift compression = τ<sub>a</sub> × [2Np-1], and *neutralized* drift compression lengths = 1000 m . Fast time-dependent correction coils assumed to compensate 2/3 of coherent velocity tilt before final focus.



# In the ModSoLinac systems analysis, source and target constraints on both transverse and longitudinal emittance were included systematically

"Net perveance" in plasma-filled chambers  $Q_c(q, A, np_{nb}) := 1.1 \cdot 10^{-3} \cdot q \cdot [A \cdot (np_{nb} + 1)]^{-1}$  where  $np_{nb}$  =plasma/ beam density ratio ave. over chamber

"Typical" example parameters, (e.g., baseline Snowmass): the ion charge state  $q := 1$

focal length  $L_f := 6$  (m), focus magnet length  $L_{mag} := 0.6$  (m) spot size  $r_s := 2 \cdot 10^{-3}$  (m) and angle  $\theta_f := 15 \cdot 10^{-3}$  (rad), normalized momentum spread  $\delta p_p := 4 \cdot 10^{-3}$  and  $np_{nb} := 0$  (no plasma between plasma plug and target).

$$\epsilon(q, A, L_f, \theta_f, r_s, np_{nb}) := r_s \cdot \sqrt{\theta_f^2 + \left[ \frac{2 \cdot q \cdot m_e}{A \cdot M_p \cdot (np_{nb} + 1)} \right] \cdot \ln \left( \frac{L_f \cdot \theta_f}{r_s} \right)}$$

Max emittance for given target spot radius  $r_s$  including effect of magnetic pinching

Emittance allowed for accelerator  $\epsilon_{na}$ , after subtracting off chromatic aberrations ( $\delta p_p$ ), geometric aberrations, and emittance growth (allowing more complete plasma-filled chambers if  $np_{nb} \gg 1$  [Welch, et.al., Phys. of Plas. 9 (2344)])

$$\epsilon_a(q, A, L_f, \theta_f, r_s, \delta p_p, np_{nb}) := \sqrt{\epsilon(q, A, L_f, \theta_f, r_s, np_{nb})^2 + \left[ \left( 2 \cdot L_f \cdot \theta_f^2 \cdot \delta p_p \right)^2 + \left[ 1.4 \cdot \left( \frac{L_f^2}{L_{mag}} \right) \cdot \theta_f^4 \right]^2 + \left( 0.5 \cdot Q_c(q, A, np_{nb}) \cdot L_f \right)^2 \right]}$$

Eq.0

With this assumed longitudinal beam energy spread out of the injector, we can estimate the resulting final beam momentum spreads after pre-bunch compression, acceleration, and drift compression to the target. To give some allowance for the growth of longitudinal momentum spread due to jitter in induction gaps and longitudinal beam control during acceleration, we will double the final momentum spread calculated from the injector with overall bunch compression.

$$\delta p_{pf}(T_f, A, q, V_o, \delta V_{V_o}, \tau_a, \tau_f, k) := \delta V_{V_o} \cdot \left( \frac{q \cdot V_o}{T_f} \right) \cdot \left( \frac{\tau_o(T_f, A, q, V_o, \tau_a, k)}{\tau_f} \right)$$

$\delta V_{V_o} := 10^{-3}$

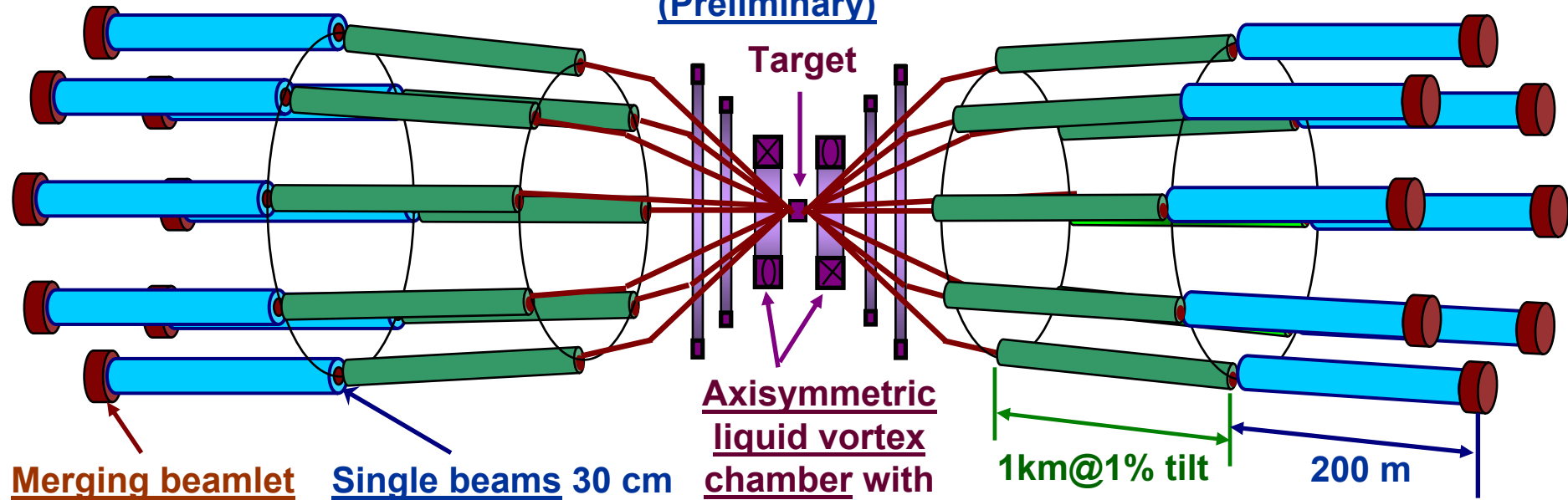
**Eq.10:**  $\delta p/p$  thermal at the target. Note factor of 2 for assumed growth in accelerator cancels the factor of 2 in  $\delta E/E=2\delta v/v$



Modular-solenoid driver example with plasma-filled vortex-cusp chamber (12-9-02)

16 -module solenoid driver (eight per end), 32 pulses for total 6.4 MJ of 2.5 GeV Xe<sup>+8</sup> ions, 7,000 tons of induction cores, 4000 solenoids, \$750 M total capital cost

(Preliminary)



Merging beamlet source/injector  
3MV, 24MeV Xe<sup>+8</sup>  
83 A/beam @ 8μs  
followed by 8x  
beam bunch  
compression

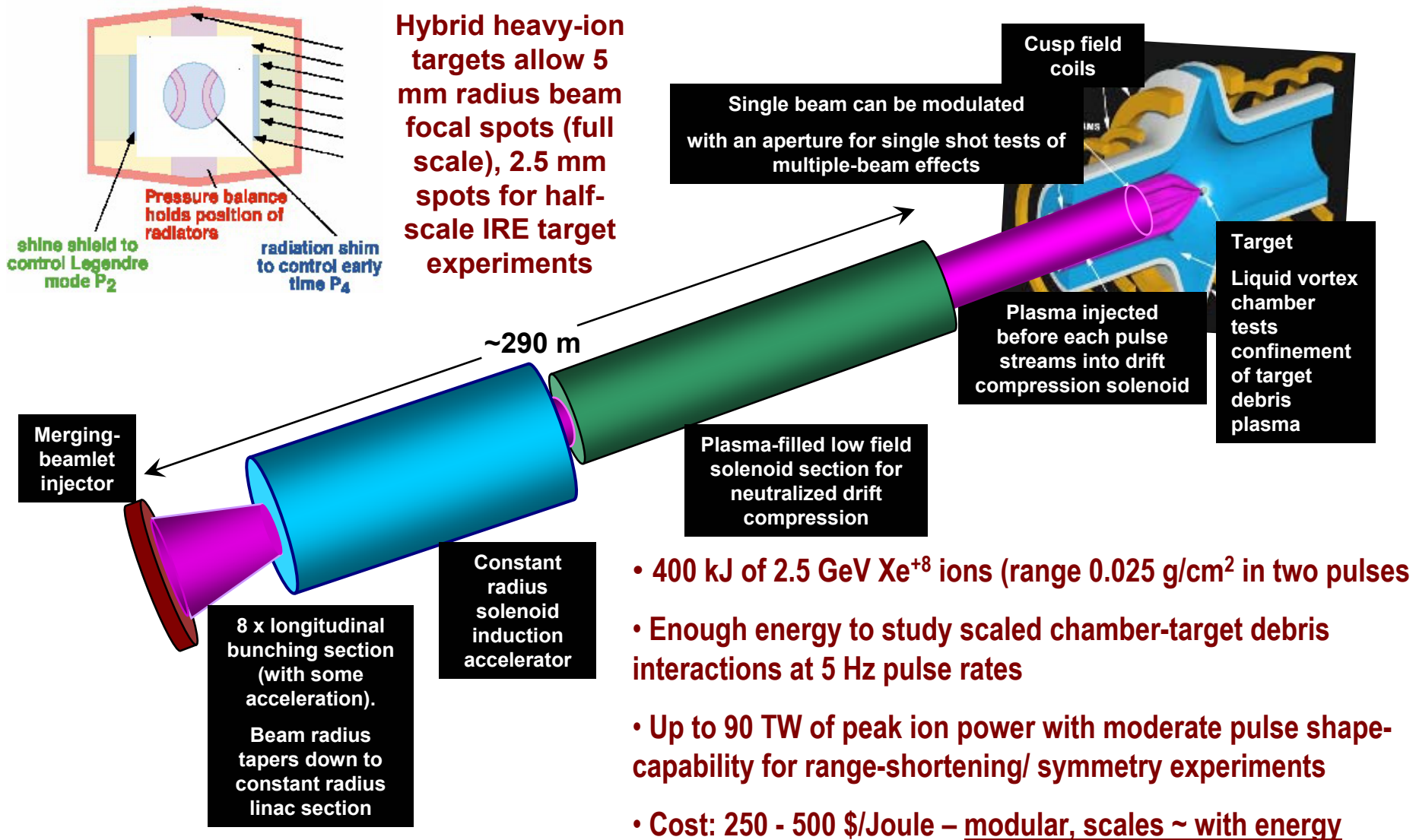
Single beams 30 cm constant diameter,  
9T solenoid, double-pulse induction for foot and main pulses,  
6.7 kA peak mp @ 2.5 GeV, 100 ns

Axisymmetric liquid vortex chamber with cusp focusing  
(dense plasma filled for Xe<sup>+8</sup> @ 9 ns). Other possibilities

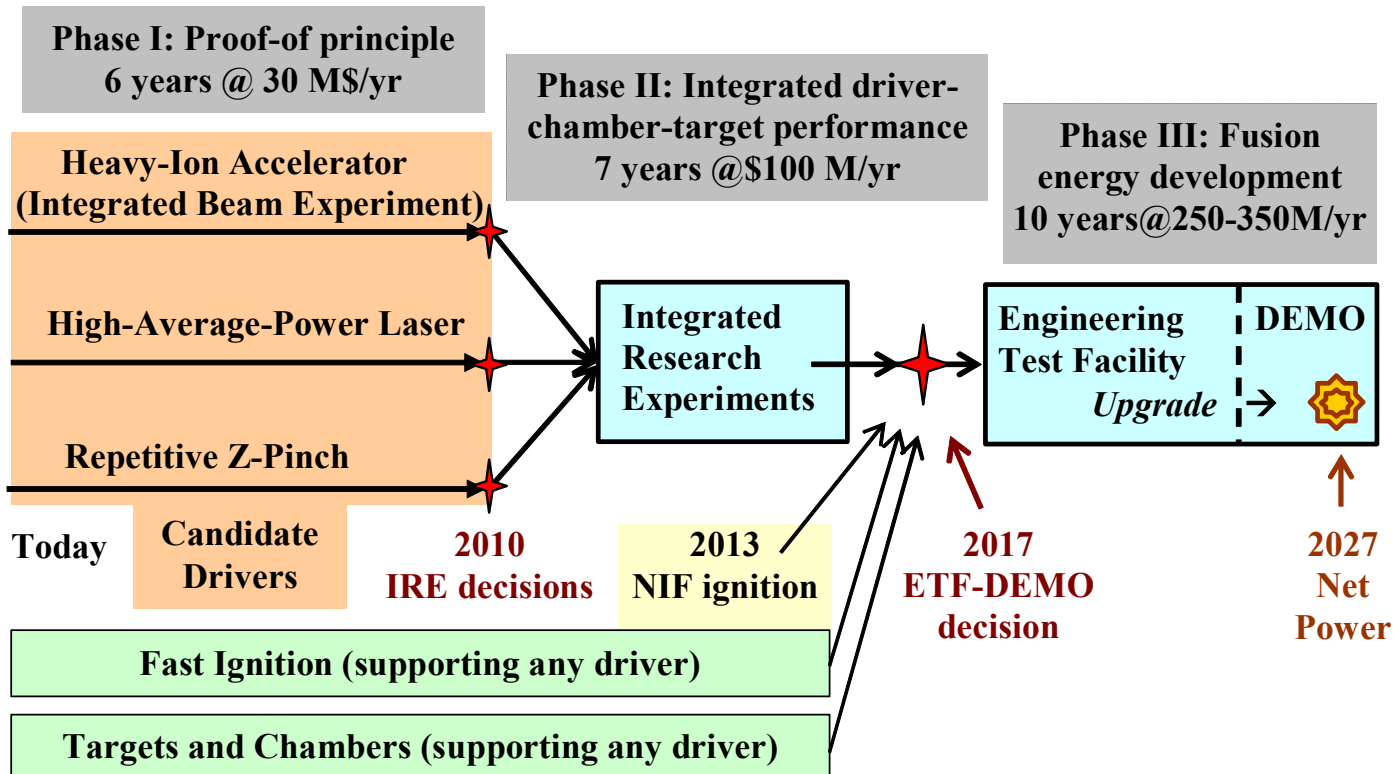
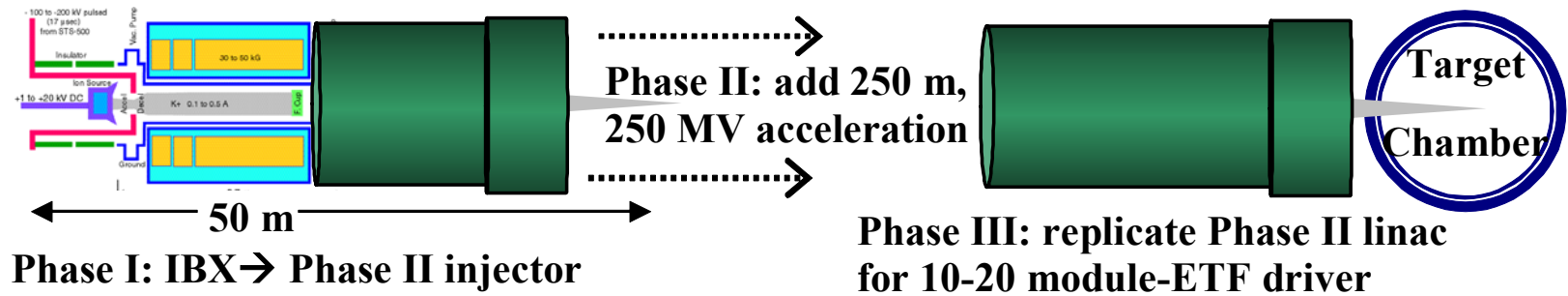
Neutralized drift compression with double pulses (foot and main pulses through each low field ~0.5 T solenoid drift line

*Detailed work may or may not confirm feasibility or cost of this preliminary example*

**Development Path:** large-focal spot HIF target designs might enable a single-beam IRE to validate one full driver module that supports a variety of integrated focus/chamber/target experiments



# Modular linacs → faster, lower cost HIF development path?



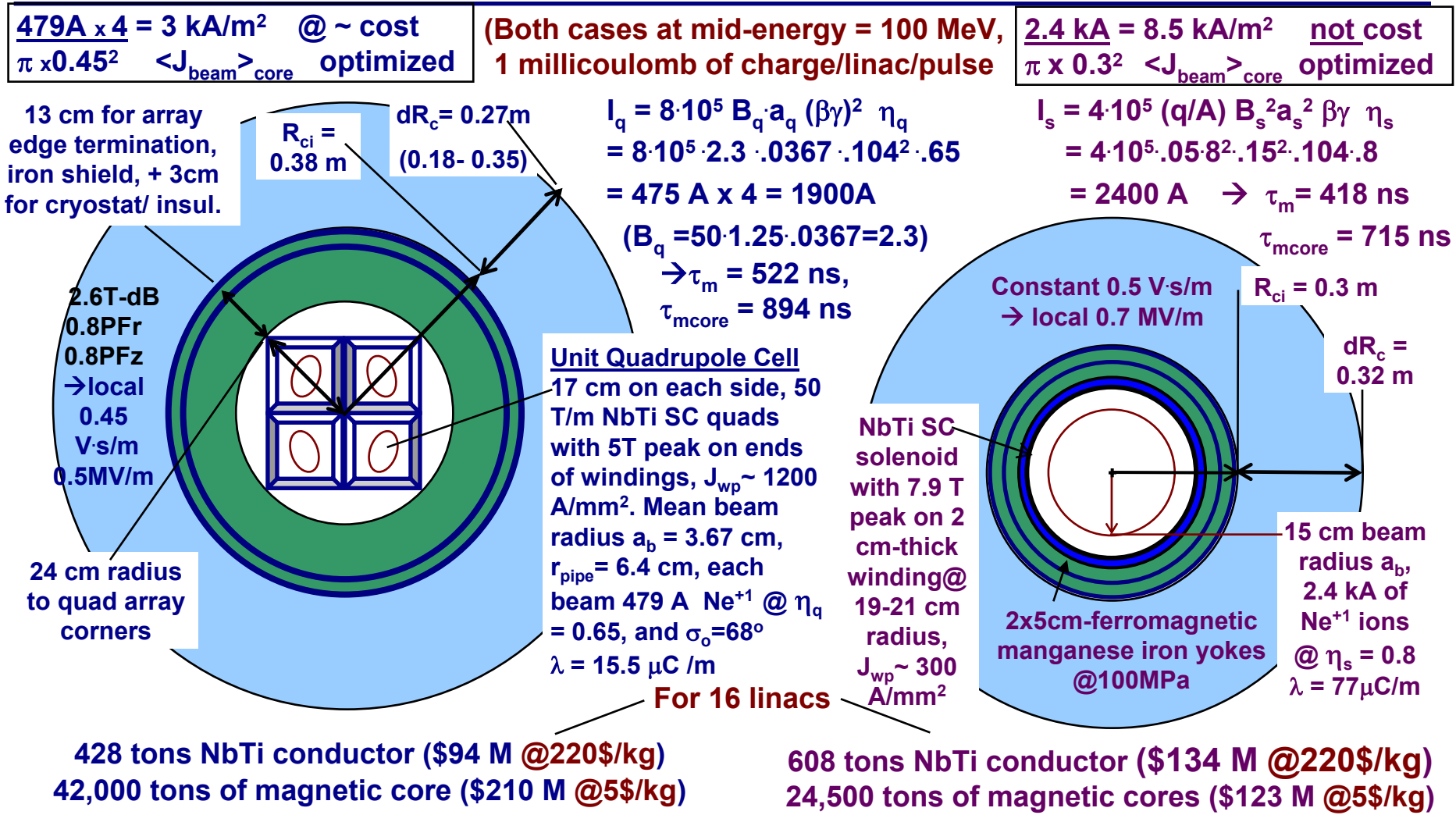
# Linac options: Solenoids, quads, or combination options may support modular HIF pathways, assuming high q/A ions can be injected and focused:

---

Lets take a closer look comparing solenoid and quadrupole transport options for a modular linac driver system driving a **6.4 MJ, 5 mm-spot-radius Hybrid target:**

- Assume double pulsing is cost-effective when pulsed power modules drive a set of 10 or more induction modules in parallel at each z.
- Consider Neon<sup>+1</sup> @ 200 MeV (Similar range as 4 GeV Bi) → 20 x lower linac voltage.
- Lowest modular system cost → smallest number of modules consistent with symmetry requirements (8 for azimuthal symmetry each end for hybrid targets). Assume double pulses meet pulse shape → 16 modules, minimum
- → 200 kJ per pulse per module for 16 modules → 1 mC charge/pulse

# Comparison: constant- $R_{ci}$ modular linac cross sections: left- 4-beam quad-array module; right: single-beam solenoid module (both $Ne^{+1}$ , 16 linac modules, double-200kJ pulses)



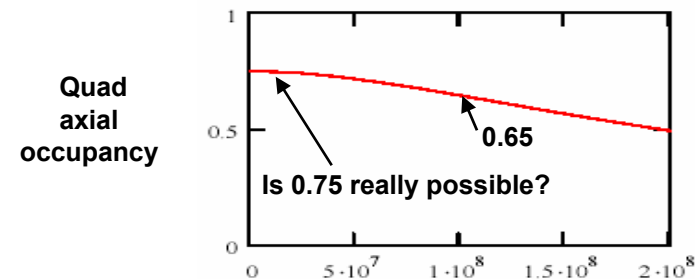
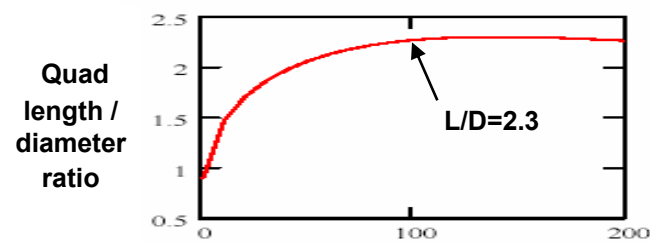
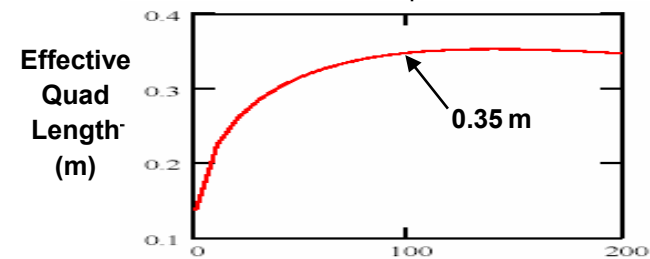
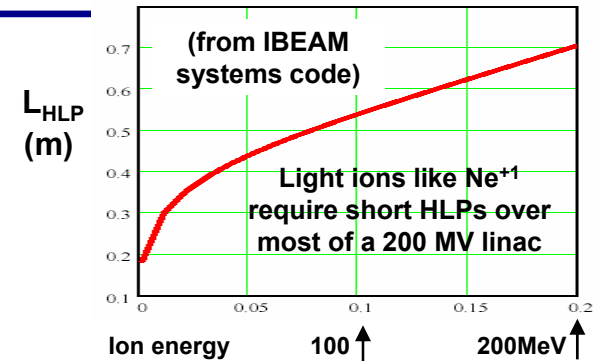
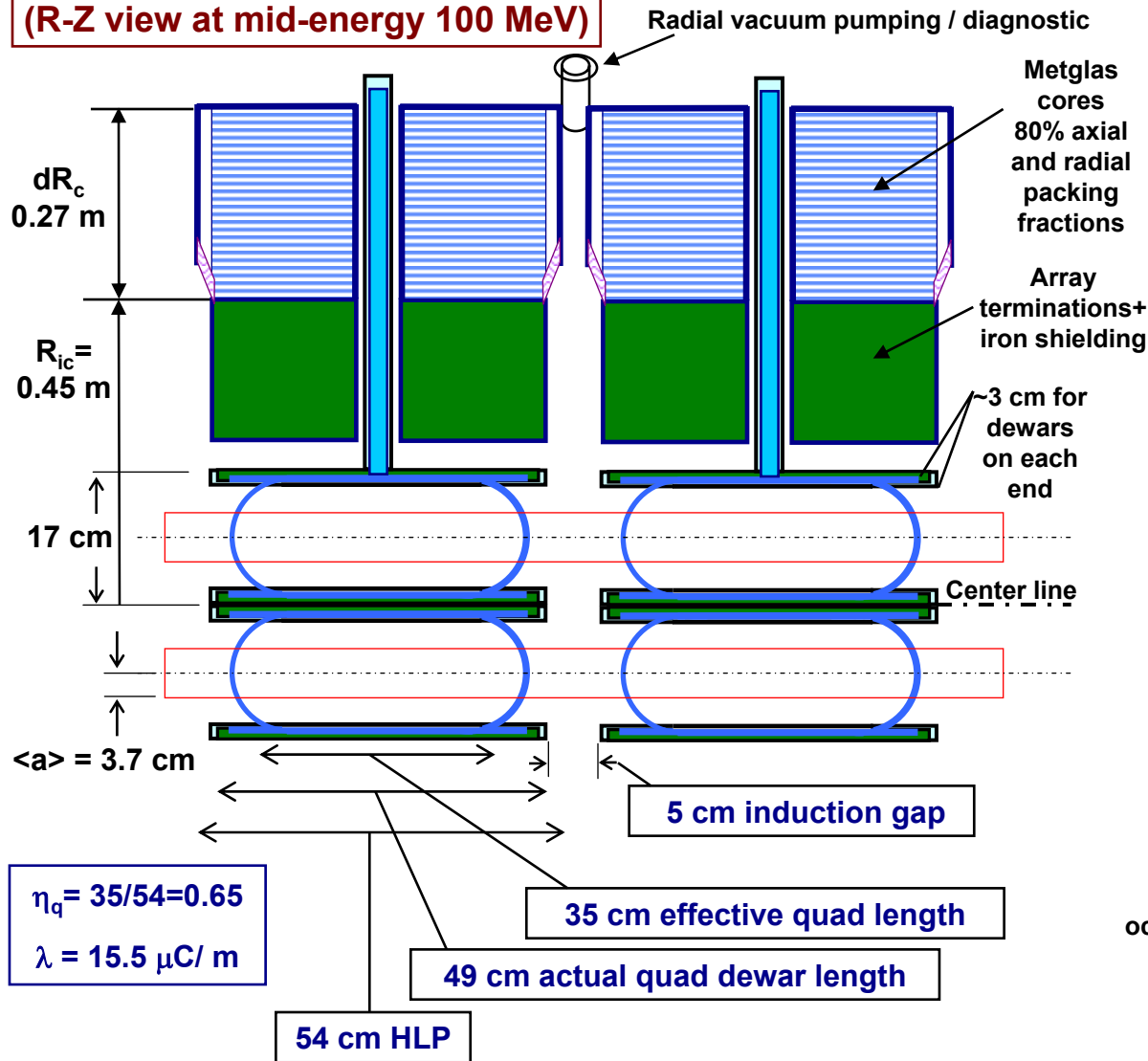
4-beam quadrupole linac module, 960 m long  
(based on IBEAM system code)

Solenoid linac module, 370 m long



# Quadrupole linacs with high $q/A$ ions like $\text{Ne}^{+1}$ require short quads (reduced effective occupancy), and low acceleration gradients

(R-Z view at mid-energy 100 MeV)



# Solenoid R-Z cross section: judicious use of ferromagnetic steels inside cores and at ends minimize stray flux into induction cores

(R-Z view at mid-energy 100 MeV)

1 m

Radial vacuum pumping and diagnostic access

Extend beam beyond last induction cell far enough to force >99.9 % of the flux return through the iron

$dR_c$   
0.32 m

Metglas cores  
80% axial and  
radial packing  
fractions

$R_{ic}$   
0.3 m

15 cm beam  
 $\lambda = 77 \mu\text{C/m}$

~3 cm for dewars each end  
3+3+5.2=11.2cm winding gaps  $\rightarrow \eta_s = 0.8$

$B_z \sim 7.8 \text{ T}$

$B_z \sim 7.92 \text{ T}$

$B_z = 5.8 \text{ T}$

$E_r = 77 \text{ kV/cm}$

Ferromagnetic manganese steel cryo structure attenuates gap fringe fields

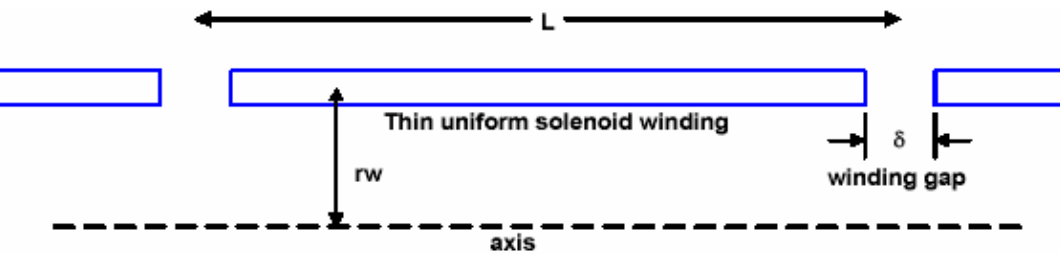
5.2 cm vacuum gap  
700 kV@135 kV/cm for 380 ns

Matthaeus finds < 0.1 T solenoid fringe field (with iron inserts) in the metglas of this example  $\rightarrow$  less than 5% increase in radial build to preserve the 0.5 V-s/m

Main-end solenoid flux return

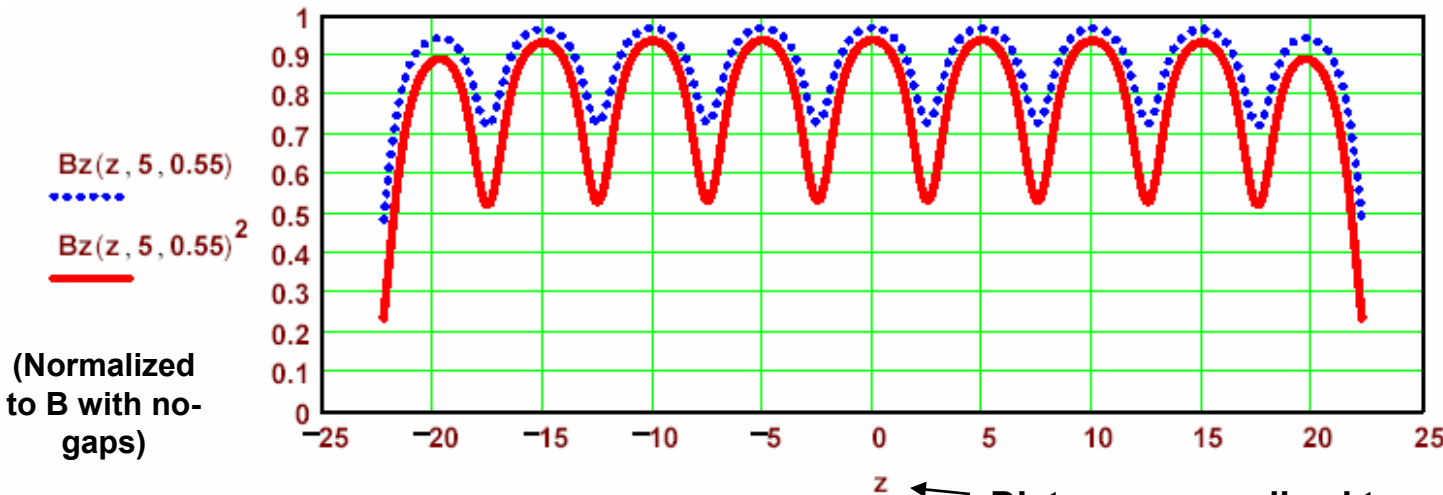
Cheap scrap-iron plates in a trench < 700\$/ton

# Effective solenoid axial occupancy $\eta_s$ based on average $B_z^2$



$B_z^2$  with gaps  $\delta$  spaced  $L$  apart, normalized to the infinite solenoid  $B_z^2$  along the axis at the same line current density ( $z$ ,  $L$ , and  $\delta$  all normalized to mean winding radius  $r_w$ )

$\eta_s(5, \delta e)$

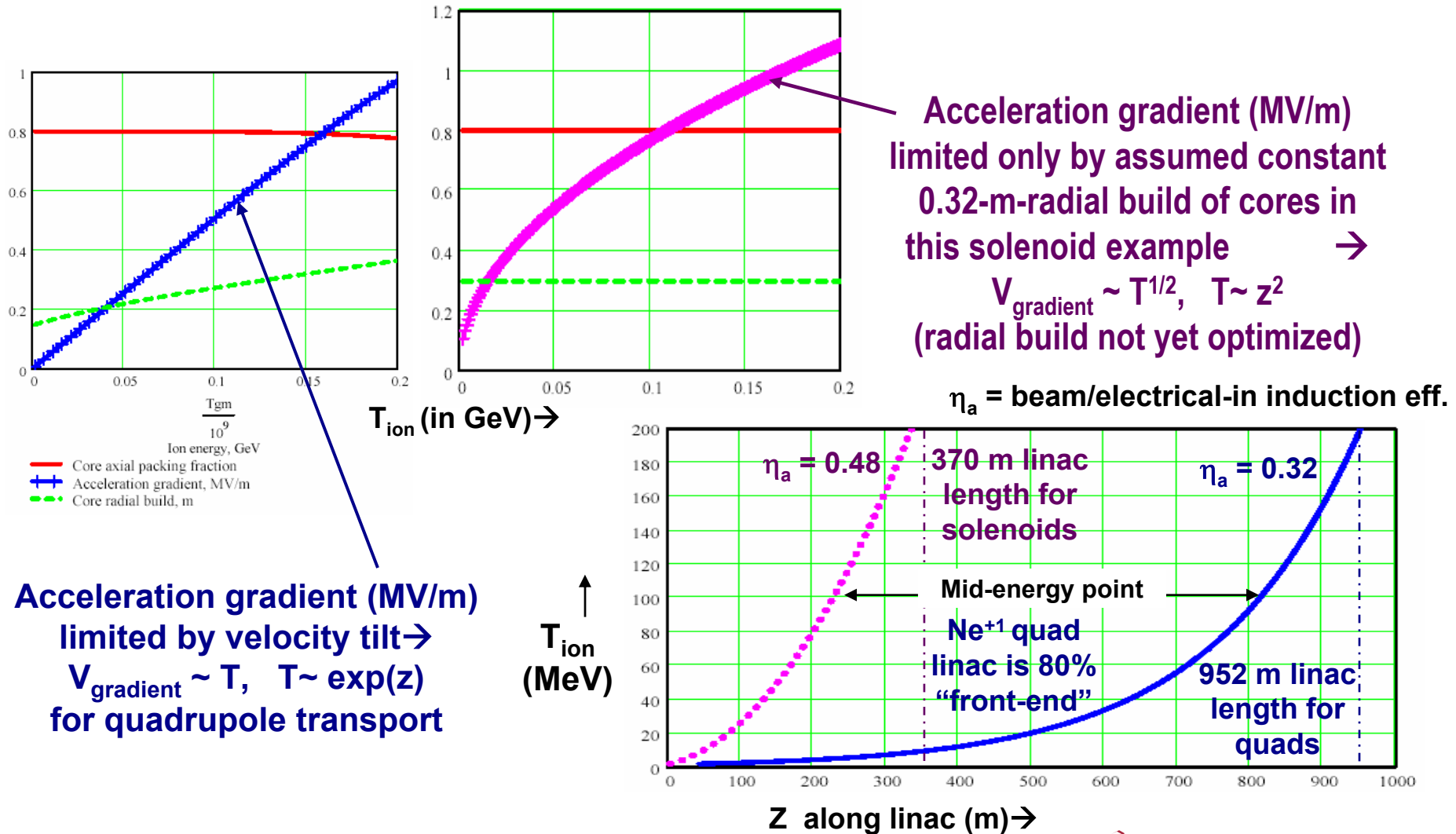


← Plot of  $B_z$  and  $B_z^2$  for a 9-HLP example with  $L=5$ ,  $\delta=0.55$ ; i.e., for  $r_w=0.2$  m  $\rightarrow$   $L=1$  m,  $\delta=11$  cm

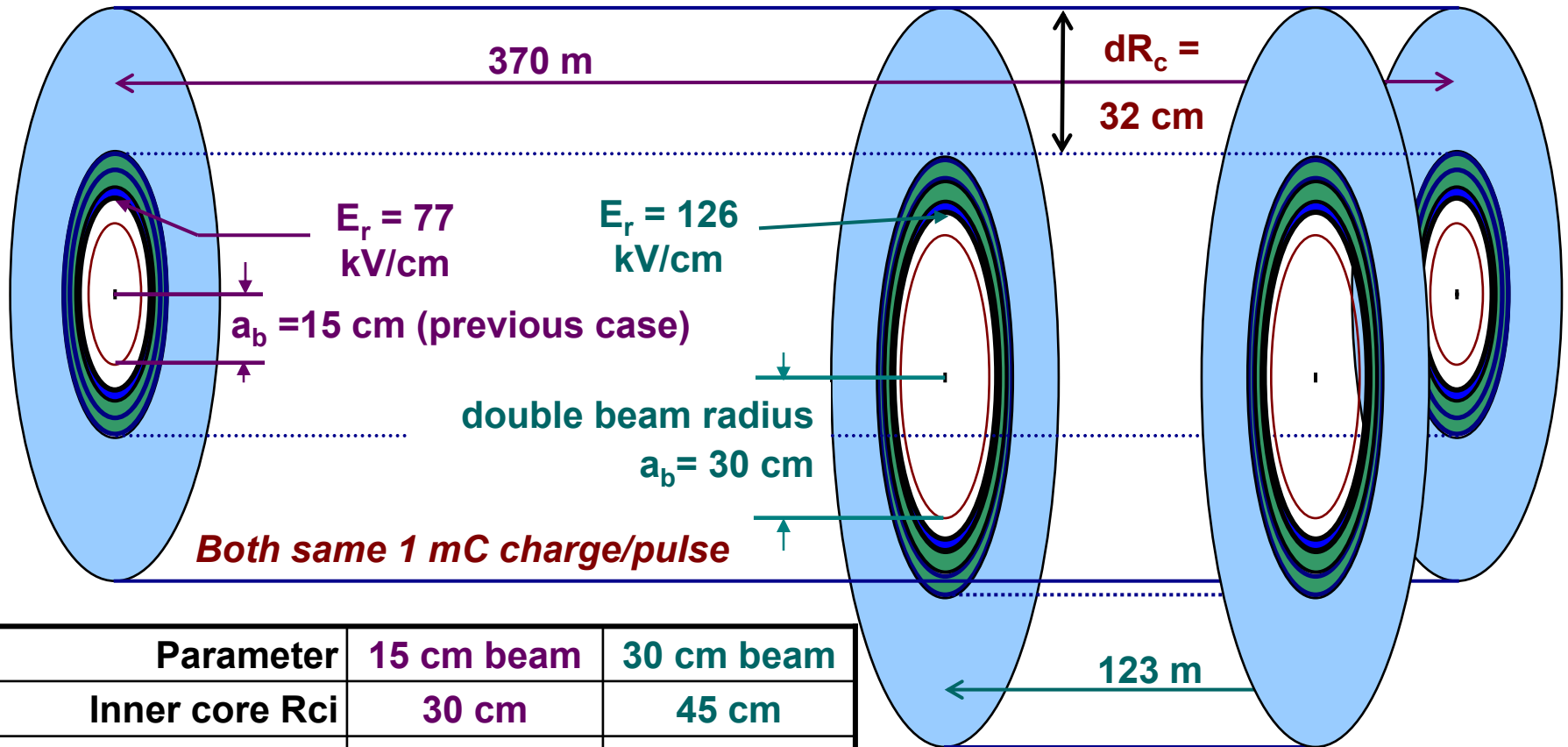
$$\eta_s(L, \delta) := \left(\frac{2}{L}\right) \cdot \int_0^{0.5 \cdot L} B_z(z, L, \delta)^2 dz \quad \eta_s(5, 0.55) = 0.797$$

Distance normalized to mean winding radius (e.g.,  $5 = 1$  m if  $r_w=0.2$  m)

**Solenoids allow different velocity head and tail ions to transport at the same radius, whereas beam radius variations constrain the maximum velocity tilt with quads → big differences in z-average acceleration gradients, and linac lengths, for modular high q/A linacs.**



Minimum cost (mass) follows  $\langle J_{bc} \cdot E_z \rangle$  better than just  $\langle J_{bc} \rangle$  -example:

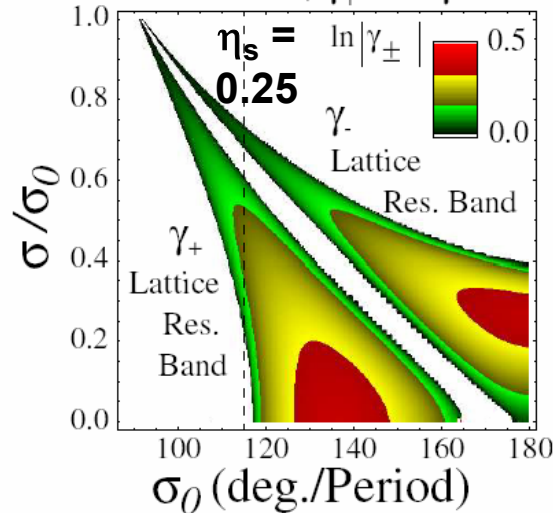
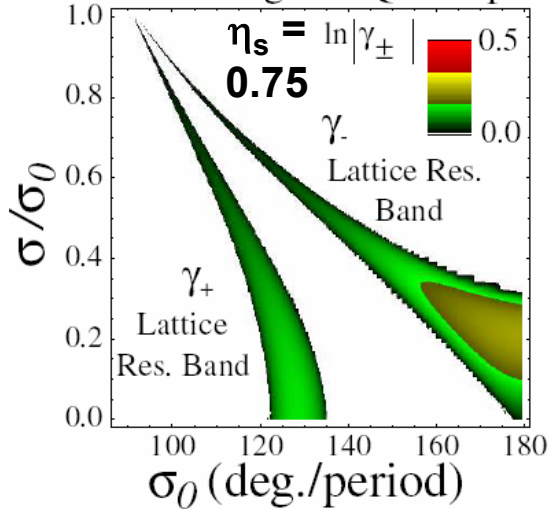


Parameter	15 cm beam	30 cm beam
Inner core Rci	30 cm	45 cm
Occupancy $\eta_s$	0.8	0.6
Core z-pack, V·s/m	0.8, 0.5 $V_s/m$	0.6, 0.38 $V_s/m$
Current @100MV	2400 A	7200 A
Pulse $\tau_m, \tau_{mcore}$	418, 715 ns	140, 240 ns
Gradient@100MV	0.7 MV/m	2.1 MV/m

Parameter	15 cm beam	30 cm-beam
Core mass	24,500 tons	7600 tons
$\langle J_{bc} \rangle$	8.5 kA/m <sup>2</sup>	11.3 kA/m <sup>2</sup>
$\langle J_{bc} \cdot E_z \rangle$	6 GW/m <sup>3</sup>	24 GW/m <sup>3</sup>

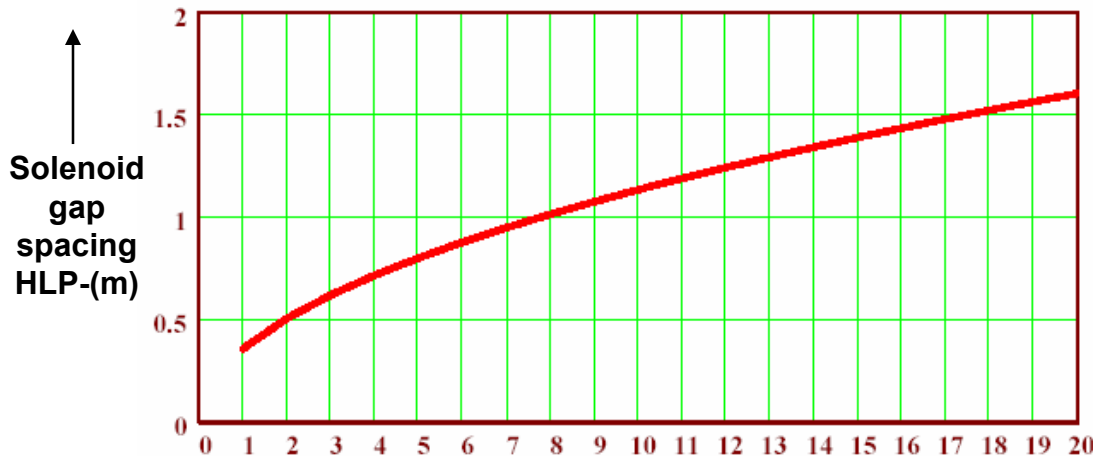


# Breathing and Quadrupole Mode Growth Factors, $\gamma_+$ and $\gamma_-$



The envelope instability bands (upper plots from Steve Lund) for solenoid transport can be avoided with high  $\eta_s$  occupancy factors and keeping phase advances  $\sigma_0 < 127$  degrees (short enough solenoid gap HLP spacing vs acceleration voltage—see lower plot from Ed Lee)

$$S_{\text{hlp}}(q, A, V, B) := \frac{7.4}{B} \cdot \sqrt{V \cdot \frac{A}{q \cdot 133}} \quad q := 1 \quad A := 20 \quad B := 8$$



Acceleration voltage V (MV)→

# Vacuum instability depends on time-average beam current and vacuum pumping speed inside pump volume (e.g., in-bore cryopumping)

→ Gas in the beam tubes can build-up in time at any initial vacuum pressure when the average beam current  $I_{\text{bave}}$  exceeds a threshold value that depends on the neutral desorption coefficient  $\Gamma_o$  (neutrals desorbed per ion lost to the walls) and on the vacuum pumping speed per meter of beam tube. The threshold [W. Turner, *J.Vac.Sci.Tech. A14(4)1996*] is determined when the number of wall neutrals desorbed per meter per second from both cold ions expelled from beam-ionized gas and from beam halo ions lost to the wall exceeds the neutrals pumped per meter per second.

One can derive the threshold time-average beam current  $I_{\text{bave}}$  for gas runaway from

$$\pi r_w^2 \frac{dn_o}{dt} = n_b n_o \sigma_i v_b \pi a_b^2 \Gamma_{og} + n_b n_o \sigma_x v_b \pi a_b^2 \Gamma_{ob} + n_b v_b \pi a_b^2 f_{hl} \Gamma_{ob} - 2\pi r_w f_{wp} n_o v_o / 4 = 0$$

and using  $I_{\text{bave}}/q e = n_b v_b \pi a_b^2$ , where  $r_w$  is the "pumping" wall radius,  $n_o$  the gas density,  $n_b$  the average beam density,  $\sigma_i$  the gas ionization-by-beam cross-section,  $\sigma_x$  the beam charge exchange cross-section,  $v_b$  the beam velocity,  $a_b$  the beam radius,  $\Gamma_{og} \sim 10$  the gas desorption coefficient for lost cold ions,  $\Gamma_{ob}$  the gas desorption coefficient for lost beam ions,  $f_{hl}$  the fractional beam halo scrape-off loss per meter,  $f_{wp}$  the fraction of wall area open for vacuum pumping (through induction gaps and holes in cold-bore liners for cryo-pumping), and  $v_o$  the gas neutral thermal velocity.

The cross section for ionization of the gas by the beam is highest in the front end, falling as  $1/v_b$ :

$$\sigma_i := 4 \cdot 10^{-20} \text{ m}^2, \text{ and for beam charge exchange}$$

$$\sigma_x := 2 \cdot 10^{-20} \text{ m}^2$$

For configurations utilizing "cold-bore" in-tube cryo pumping with a 20 K perforated liner, the neutral speed is

$$v_{oc} := \sqrt{\frac{2 \cdot 20 \cdot e}{2 \cdot M_p \cdot 11600}}$$

$$v_{oc} = 406 \text{ m/sec thermal speed @ 20 degree K for H}_2$$

and the wall pumping aperture fraction

$$f_{wpc} := 0.5 \text{ at the pipe (pumping) radius } r_w \sim 0.04 \text{ m}$$

For multi-beam arrays utilizing "warm bores" (either normal quad magnets or electric quads), the neutral speed is

$$v_{oh} := \sqrt{\frac{2 \cdot 300 \cdot e}{2 \cdot M_p \cdot 11600}}$$

$$v_{oh} = 1574 \text{ m/sec thermal speed @ 300 degree K for H}_2$$

and the wall pumping aperture fraction

$$f_{wph} := 0.05 \text{ at the pumping radius } \sim 0.4 \text{ m outside the array.}$$

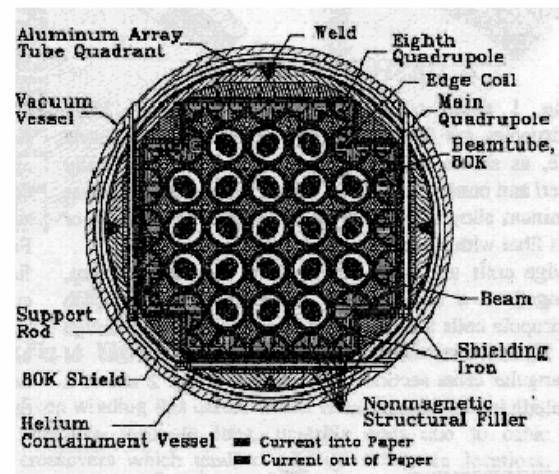
For a cold-ion reflux coef.  $\Gamma_{og} := 10$

Threshold peak current for gas runaway @5Hz

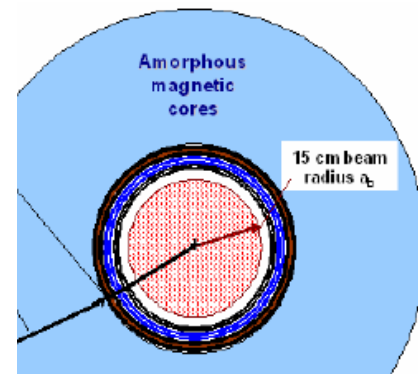
$$I_{th}(q, r_w, n_o, v_o, \sigma_x, f_{wp}, f_{hl}, \Gamma_{ob}, \tau_b) := \frac{0.5 \cdot q \cdot e \cdot \pi \cdot r_w \cdot f_{wp} \cdot n_o \cdot v_o}{n_o \cdot \sigma_i \cdot \Gamma_{og} + n_o \cdot \sigma_x \cdot \Gamma_{ob} + f_{hl} \cdot \Gamma_{ob}} \cdot \frac{2 \cdot 10^{-1}}{\tau_b} \quad \text{(A), Eq. 3}$$

where the factor on the right with pulse width  $\tau_b^{-1}$  is the inverse duty factor to get peak threshold beam current from beam currents averaged over 5 Hz pulse rates.

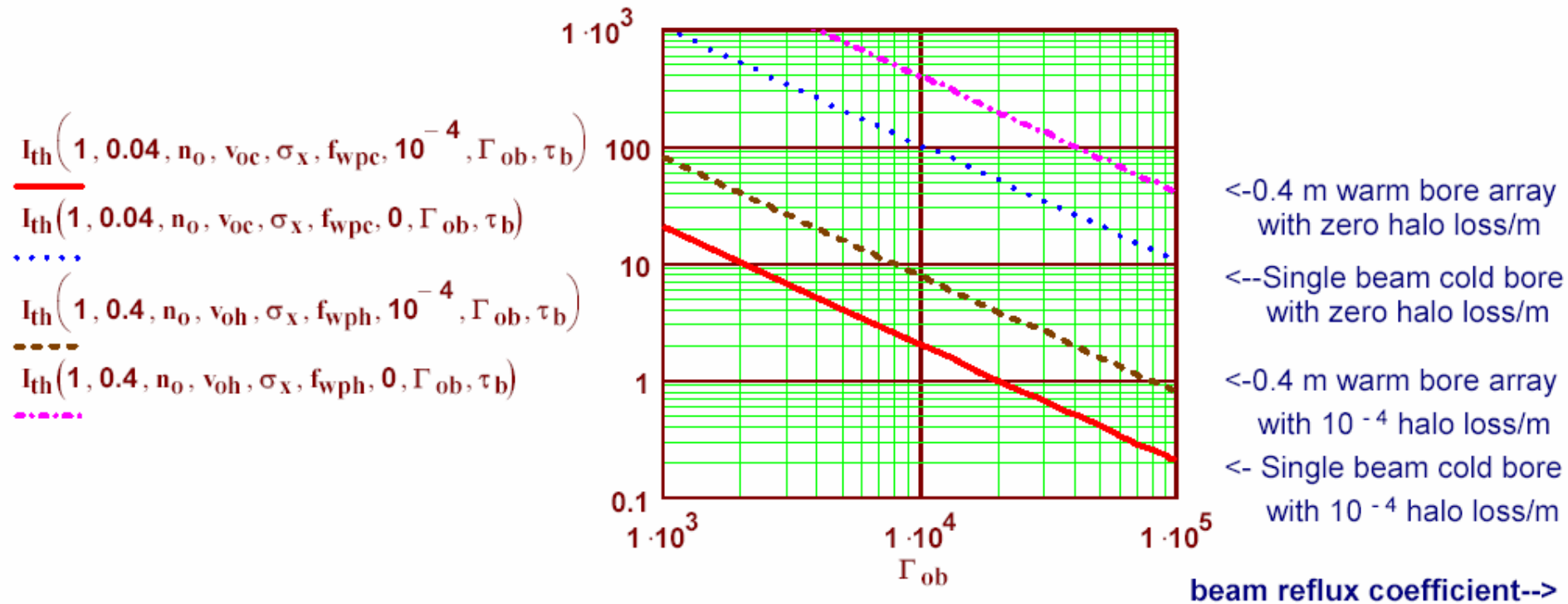
Nominal neutral density (@ $10^{-8}$  torr):  $n_o := 10^{14} \text{ (m}^{-3}\text{)}, \text{ pulse width } \tau_b := 20 \cdot 10^{-6} \text{ (s)}$



Compare threshold currents predicted by this model for multi-beam quad and single beam solenoids

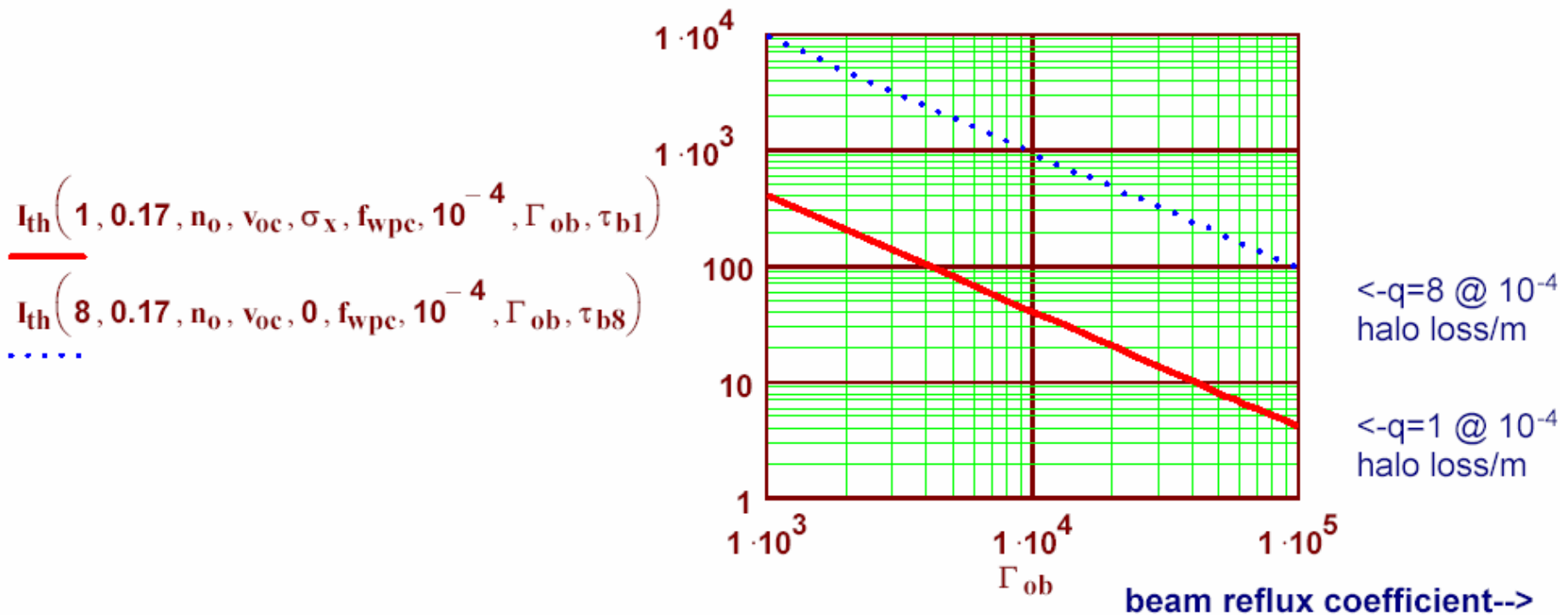


# Threshold peak current (A) for gas runaway for quads@ 5 Hz vs. neutral desorption coefficient $\Gamma_{ob}$ , for each beam w/in-bore cryo-pumping, and for total beam current w pumping at the edge of warm-bore arrays.



→ Beam currents < 2 A per beam peak @ 5Hz should be OK at  $\Gamma_{ob} < 10^4$  and  $10^{-4}$  fractional beam loss per meter with superconducting quadrupole linacs with cold-bore-cryo pumping in each beam-tube. Without cold-bore pumping in each beam tube, however, the total beam current in a warm-bore multi-beam array pumped from the outside, under the same assumptions, may be limited to < 8 A, or less than 80 mA per beam for a 100-beam array. Note in Eg 3 that threshold currents are insensitive to neutral density in the limit of either large neutral density or small halo loss  $f_{hl}$ . Use of special halo scrapers (next slide) may then be needed.

# Threshold peak current (A) for gas runaway @ 5 Hz vs. beam-neutral reflux coefficient $\Gamma_{ob}$ for single solenoid beams with cold-bore pumping, for $q = 1$ and $q = 8$ Xenon beams, with $10^{-4}/m$ halo loss.



Assume  $q = 1$  and  $q = 8$  single beams in solenoids with cold-bore cryo pumping. Since the solenoid field prevents cold ions from reaching the wall to desorb gas, we turn off the neutral reflux term by setting the ionization cross section  $\sigma_i$  to zero. For  $q=8$ , beam ions which charge exchange off gas can still be confined by the solenoid, so we turn off the cx cross-section  $\sigma_x$  as well. Threshold peak currents for gas runaway are evaluated for beam pulses of 4.3 and 1.5  $\mu\text{sec}$  for  $q = 1$  and  $q = 8$ , respectively.  $\rightarrow$  Solenoid linacs have 1-2 orders of magnitude higher beam current threshold for  $q = 1$  and  $q = 8$ , respectively, than for single beam quadrupole linacs, due to larger (17 cm) pipe radius, shorter pulses, and prevention of cold ion expulsion.



# Modular HIF development – Issues/ RD needs

**\* Needed for higher-current modular linacs using either quadrupole or solenoids transport**

- Design and validate fat- spot targets ( > 5 mm radius focal spots)\*
- Merging beamlet injectors (aberrations, and source life for higher injection currents)\*
- Agile-waveform induction modules for longitudinal beam control, bunch compression, double pulsing\*
- Tolerable stray flux (iron shield thickness) for > 95% effective core volt-seconds\*
- Emittance growth and steering/matching corrections for alignment or magnet field errors\*
- Vacuum instability control, ion stripping, halos and electron cloud effects in the linac\*
- Optimization of plasma profiles for neutralized ballistic and /or assisted pinch focusing\*
- Neutralized drift compression and final focus – long plasma pre-filled channels, long beam – plasma interaction regions, fast time-dependent /cusp/plasma lens focusing for focusing larger  $\delta p_z/p_z$ \*
- *Desirable, but not essential, for solenoids: high charge-state heavy-ion sources (laser or ECR)*

**→ The physics and technology needs for modular HIF either are being addressed or can be addressed with current VNL experimental facilities and codes**



# Backup Viewgraphs

# **What HIF needs to have a faster cheaper development path required to be competitive with other fusion approaches identified in the 3-6-03 FESAC report:**

---

- 1. A modular driver development path in which an affordable single beam IBX validates a single beam IRE which can then be replicated to create an ETF/DEMO driver on the same site.**
- 2. Heavy-ion targets with a larger spot radius  $> 5$  mm, to enable a better, faster, cheaper development path for HIF based on modular linacs. Low impedance pulsed power may also apply to modular HIF driver systems**
- 3. Thick-liquid-protected chambers, to have any realistic chance of a DEMO that works (credible lifetime and low environmental impact) in a realistic time frame ( $< 25$  years as opposed to  $> 35$  years to infinity).**

# Neutralized drift line (pg. 62-63 in ModSoLinac7.pdf)

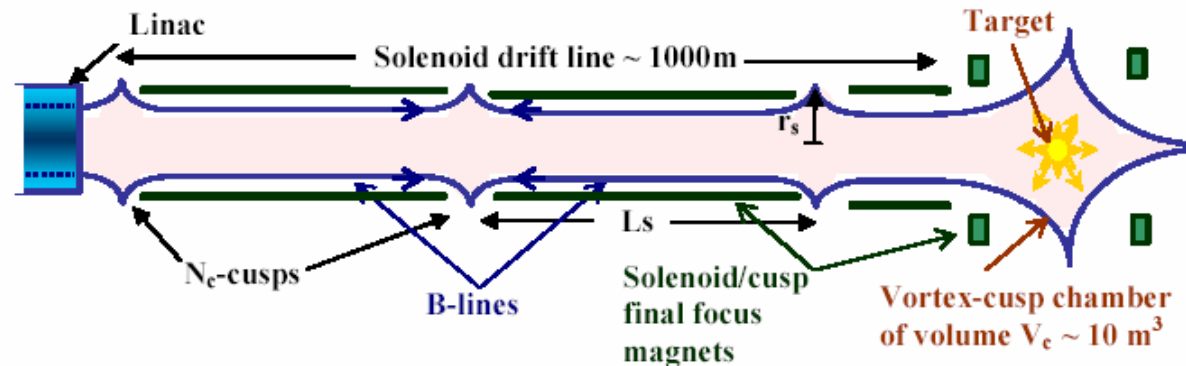
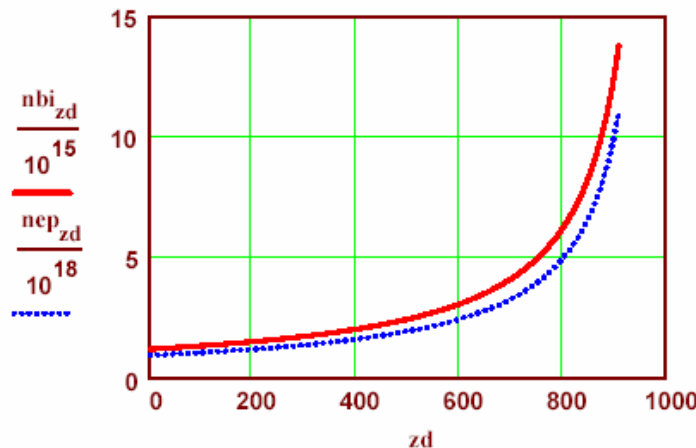


Fig. 22: A neutralized drift compression line of overall length  $L_d$  consisting of a series of long 0.5 T solenoids with alternating field polarity, forming a series of  $N_c$  cusps along the drift line. The field line curvature is stable to magnetohydrodynamic (MHD) instabilities driven by the plasma pressure-gradient. The periodic cusps may interrupt plasma return currents to stabilize or weaken two-stream modes. Plasma can be injected into the drift line either into each ring-cusp, or filled by plasma outflow to the left from the target chamber plasma.



Beam density  $n_{bi}$  displayed in units of  $10^9$  ions/cm<sup>3</sup>

Plasma electron density  $n_{ep}$  displayed in units of  $10^{12}$  electrons/cm<sup>3</sup>. Much higher densities ( $> 10^{15}$  cm<sup>-3</sup>) are required within the cusp focusing vortex chamber, where the local beam density increases due to focusing convergence.

Distance along drift compression--> (meters)

Fig. 23: Local ion beam and plasma electron densities along  $z$  for neutralized drift compression physics example.

# Target examples assumed for 10 cases selected for study

Fig 2 : (b) Target example 2  
Hybrid target, central ignition,  
two-sided illumination

$Ed_2 := 6.7 \cdot 10^6$  (J) beam input

$\tau f_2 := 9 \cdot 10^{-9}$  (s) pulse

$rs_2 := 4 \cdot 10^{-3}$  (m)

$Nm_2 := 20$  Minimum beams for symmetry and pulse shaping (5 azimuth x 2 for pulse shaping x2 sides). Assumes shim fixes range-shortening.

(Note Hybrid targets have beam angles restricted to <10 degrees --> more limited # of beams)

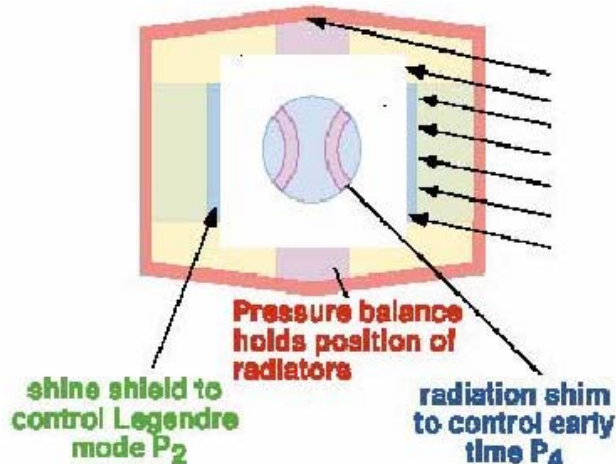


Fig 2 : (c) Target example 3  
Distributed radiator, fast ignition,  
one-sided illumination.

$Ed_3 := 4 \cdot 10^6$  (J) ion beam input

$\tau f_3 := 28 \cdot 10^{-9}$  (s) pulse

$rs_3 := 4 \cdot 10^{-3}$  (m)

$Nm_3 := 20$  Min # pulses= 5 azimuth x 2 energies x 2 pulse shape x 1 side)

Requires 600 kJ igniter beam input for 120 eV hohlraums. Might use P4 shims for symmetry: single ion energy?

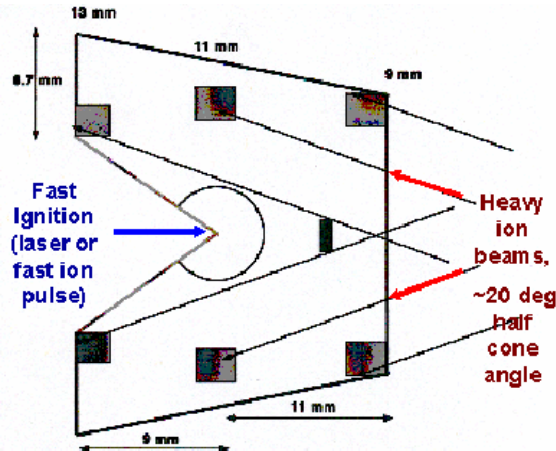


Fig 2 : (e) Target example 5  
"Tuna-can" target, fast ignition,  
one-sided illumination

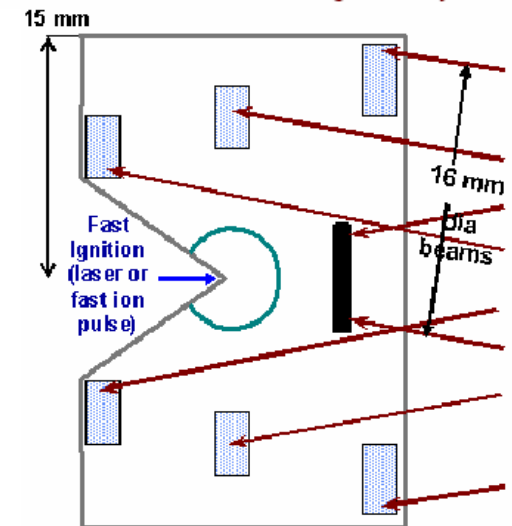
$Ed_5 := 6 \cdot 10^6$  (J) ion beam input

$\tau f_5 := 28 \cdot 10^{-9}$  (s) pulse

$rs_5 := 8 \cdot 10^{-3}$  (m)

$Nm_5 := 20$  Min # ion pulses @ <12 deg, low compression, and big case/capsule ratio  
5 azimuth x 2 energies x 2 for pulse shaping x 1 side

Requires 600 kJ igniter beam input for 120 eV hohlraums. Might use P4 shims to aid in symmetry: single ion energy? Poor coupling efficiency, but maximum beam spot at 6 MJ to explore lower cost solenoid driver options. May use bigger capsule, higher 1 GJ yield



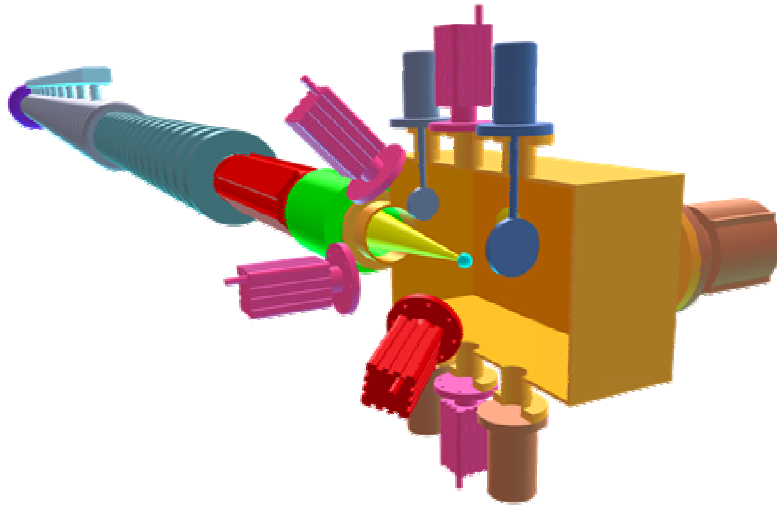
# Modular Solenoid Linacs – Opportunities/ Motivation:

---

- Transport driver charge and energy in reasonable  $N = 10$  to  $20$  modular linacs  
→ development path: single - beam IRE fully validates a driver
- Magnetic compression pulsers can drive  $N$  -linacs in parallel (cost efficient)
- Simpler single beam linac construction, vacuum /cryo access, and maintenance
- Solenoid field geometry prevents wall secondary electron ingress
- Potential 3 x lower total driver system mass and cost

**All IBX options must satisfy the same IBX science mission:  
*Provide integrated source-to-target physics experiments  
with a single high-current heavy ion beam of IFE-relevant  
brightness to optimize target focusing.***

---



In addition to the science mission, we would like any IBX option to provide sufficient proof-of-principle tests to validate corresponding IRE and driver concept (s); at minimum to include:

- Sufficient beam line-charge in accelerator ( $\sim$ current HCX- $\lambda$ ) for gas/electron physics.
- Sufficient acceleration to achieve  $>10 \times$  longitudinal bunch compression in  $< 40$  m.
- Focusing into a well-diagnosed plasma-neutralizing chamber (ballistic neutralized and assisted pinch focusing experiments).

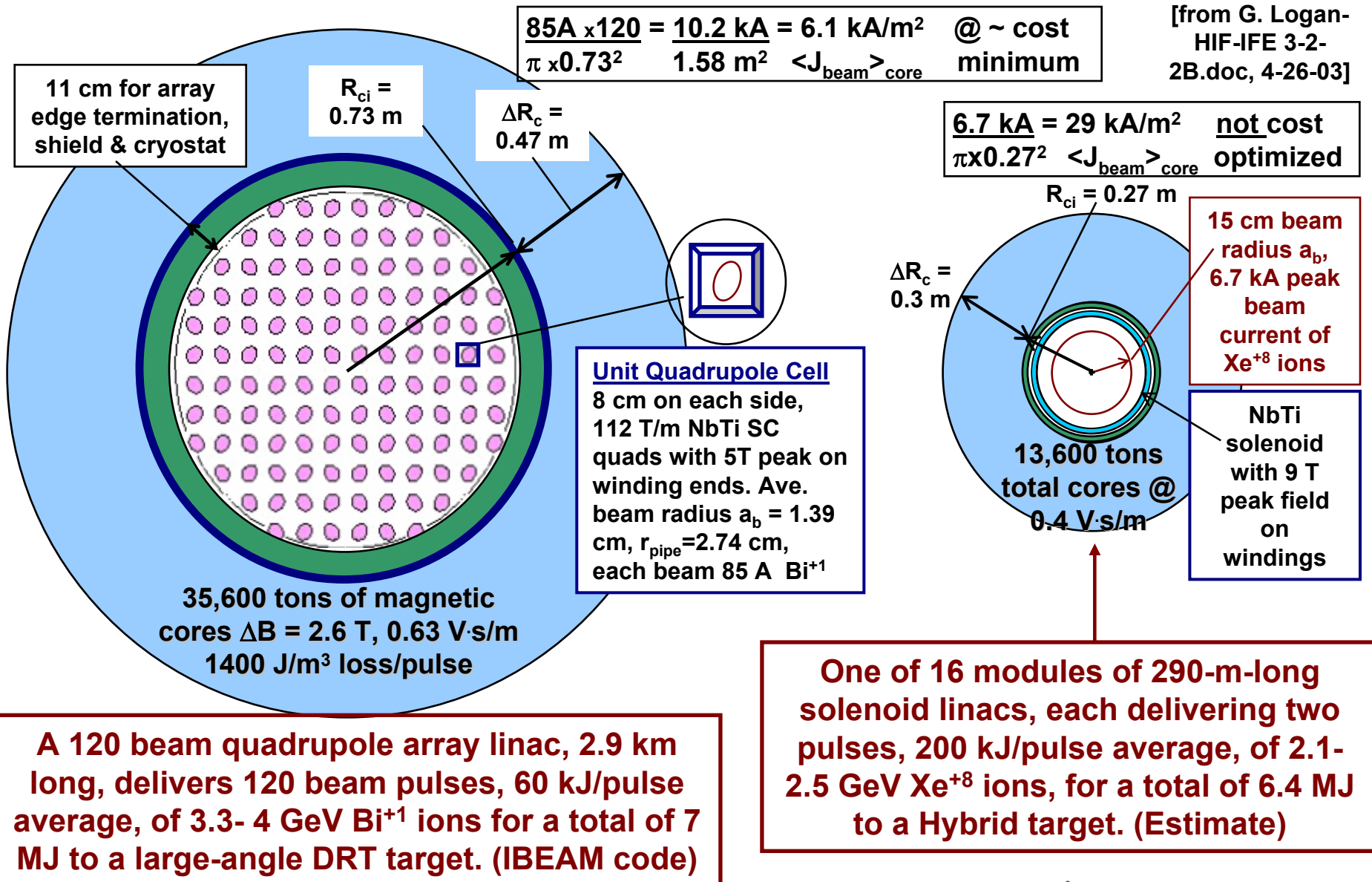
✓To avoid lethal DOE “sticker-shock reactions”, I ask the IBX TPC (MDF or MIE cost) of any option not to exceed the 4-18-03 cost maximum of \$80M including R&D) to achieve any minimum proof-of-principle experiment.

✓Lower cost IBX options could *expedite possible IBX schedules in OFES*.

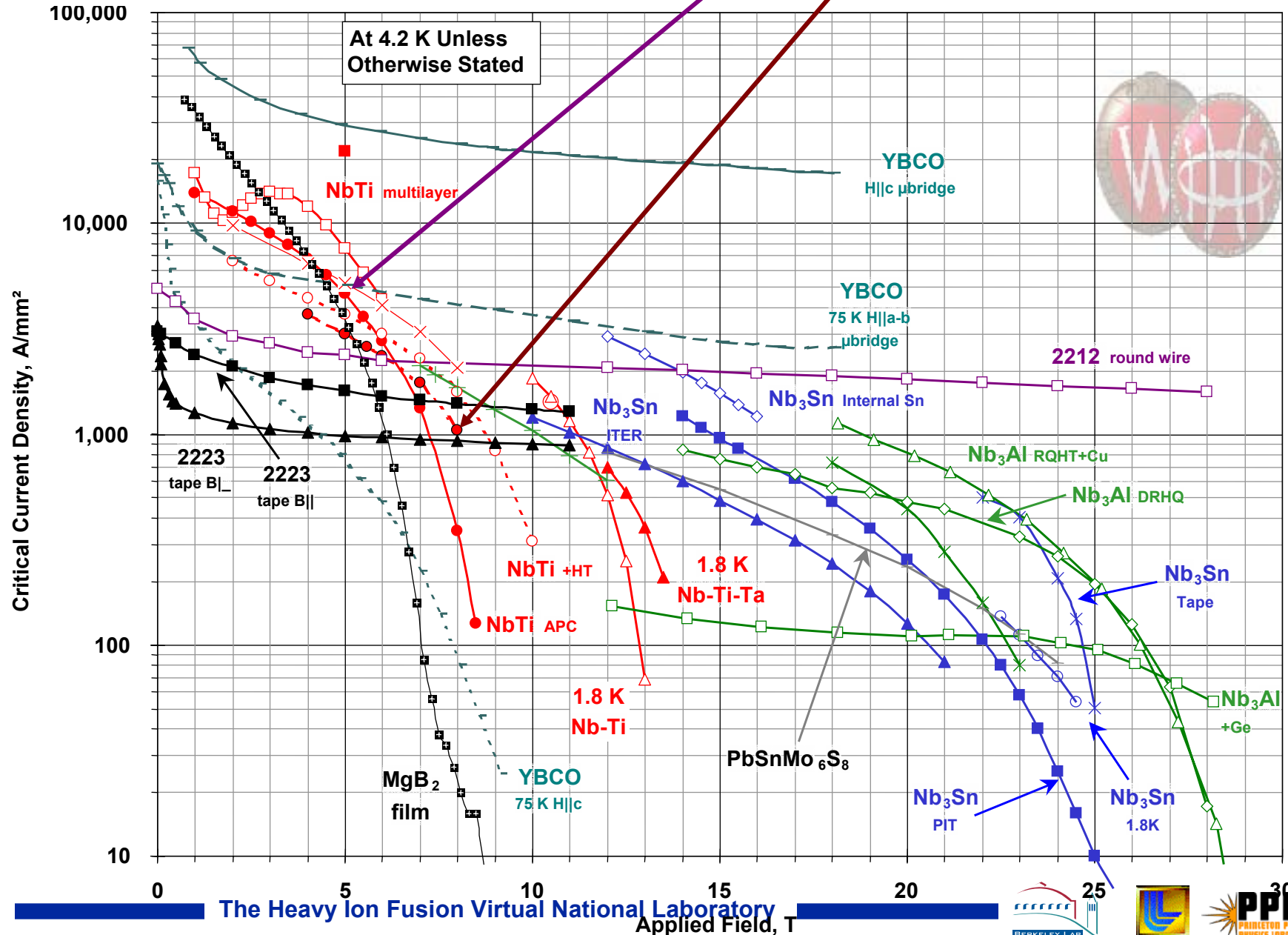
✓Can allow  $\sim$ \$30 M max additional upgrades over a 6-year operating program.



# First comparison: constant radius induction linac cross sections: left- RPD 120-beam quad-array linac; right: single-beam solenoid linac (one of 16 modules, double-pulsed)



# The optimal type of NbTi conductor for 8 T is DIFFERENT that the optimal type for 5T



# Legend

—□— Nb-Ti: Nb-Ti/Nb (21/6) 390 nm multilayer '95 (5°), 50  $\mu\text{V}/\text{cm}$ , McCambridge et al. (Yale)

—■— Nb-Ti: Nb-Ti/Ti (19/5) 370 nm multilayer '95 (0°), 50  $\mu\text{V}/\text{cm}$ , N. Rizzo et al. LTSC'96 (Yale)

—●— Nb-Ti: APC strand Nb-47wt.%Ti with 24vol.%Nb pins (24nm nominal diam.) - Heussner et al. (UW-ASC)

—×— Nb-Ti: Aligned ribbons, B|| ribbons, Cooley et al. (UW-ASC)

- - - ○ - - - Nb-Ti: Best Heat Treated UW Mono-Filament. (Li and Larbalestier, '87)

- - - ● - - - Nb-Ti: Example of Best Industrial Scale Heat Treated Composites ~1990 (compilation)

—○— Nb-Ti(Fe): 1.9 K, Full-scale multifilamentary billet for FNAL/LHC (OS-STG) ASC'98

—△— Nb-Ti: Nb-47wt.%Ti, 1.8 K, Lee, Naus and Larbalestier UW-ASC'96

—▲— Nb-44wt.%Ti-15wt.%Ta: at 1.8 K, monofil. high field optimized, unpubl. Lee, Naus and Larbalestier (UW-ASC) '96

—▲— Nb<sub>3</sub>Sn: Bronze route int. stab. -VAC-HP, non-(Cu+Ta) J<sub>c</sub>, Thoener et al., Erice '96.

—■— Nb<sub>3</sub>Sn: SMI-PIT, non-Cu J<sub>c</sub>, 10  $\mu\text{V}/\text{m}$ , 36 filament 0.8 mm dia. (42.6% Cu), U-Twente & NHFML data provided April 29th 1999

—\*— Nb<sub>3</sub>Sn: Tape (Nb,Ta)<sub>6</sub>Sn<sub>5</sub>+Nb-4at.%Ta core, [J<sub>c,core</sub>, core ~25 % of non-Cu] Tachikawa et al. '99

—○— Nb<sub>3</sub>Sn: Bronze route VAC 62000 filament, non-Cu 0.1  $\mu\Omega/\text{m}$  1.8 K J<sub>c</sub>, VAC/NHFML data courtesy M. Thoener.

—◇— Nb<sub>3</sub>Sn: Non-Cu J<sub>c</sub> Internal Sn OI-STI RRP #6555-A, 0.8mm, LTSW 2002

—△— Nb<sub>3</sub>Al: RQHT+2 At.% Cu, 0.4m/s (Iijima et al 2002)

—\*— Nb<sub>3</sub>Al: Nb stabilized 2-stage JR process (Hitachi,TML-NRIM,IMR-TU), Fukuda et al. ICMC/ICEC '96

—◇— Nb<sub>3</sub>Al: DRHQ with Intermediate cold-work, core J<sub>c</sub>, Kikuchi et al. (NRIM) ASC2000

—□— Nb<sub>3</sub>Al: 84 Fil. RHQT Nb/Al-Ge(1.5  $\mu\text{m}$ ), Iijima et al. NRIM ASC'98 Paper MVC-04

—+— Nb<sub>3</sub>Al: JAERI strand for ITER TF coil

—■— YBCO: /Ni/YSZ ~1  $\mu\text{m}$  thick microbridge, H||c 4 K, Foltyn et al. (LANL) '96

—■— YBCO: /Ni/YSZ ~1  $\mu\text{m}$  thick microbridge, H||ab 75 K, Foltyn et al. (LANL) '96

- - - ■ - - - YBCO: /Ni/YSZ ~1  $\mu\text{m}$  thick microbridge, H||c 75 K, Foltyn et al. (LANL) '96

—□— Bi-2212: non-Ag J<sub>c</sub>, 427 fil. round wire, Ag/SC=3 (Hasegawa ASC2000+MT17-2001)

—■— Bi 2223: Rolled 85 Fil. Tape (AmSC) B||, UW'6/96

—▲— Bi 2223: Rolled 85 Fil. Tape (AmSC) B||, UW'6/96

—+— PbSnMo<sub>6</sub>S<sub>8</sub> (Chevrel Phase): Wire in 14 turn coil, 4.2 K, 1  $\mu\text{V}/\text{cm}$ , Cheggour et al., JAP 1997

—■— MgB<sub>2</sub>: "low oxygen" film 3, Eom et al. (UW) Nature 31 May

# GianLuca recommended two NbTi conductors for 8T

**Table 5 Comparison of critical current densities for SSC Sumitomo strand and IGC-AS strands**

Field	Sumitomo SSC 4.2K	IGC 7363 1-1-7 at 4.2K
5	2767	3062
7	1748	1765
7.5		1463
8	956	1154
5T/7T	1.58	1.735107731
5T/8T	2.89	2.653100775

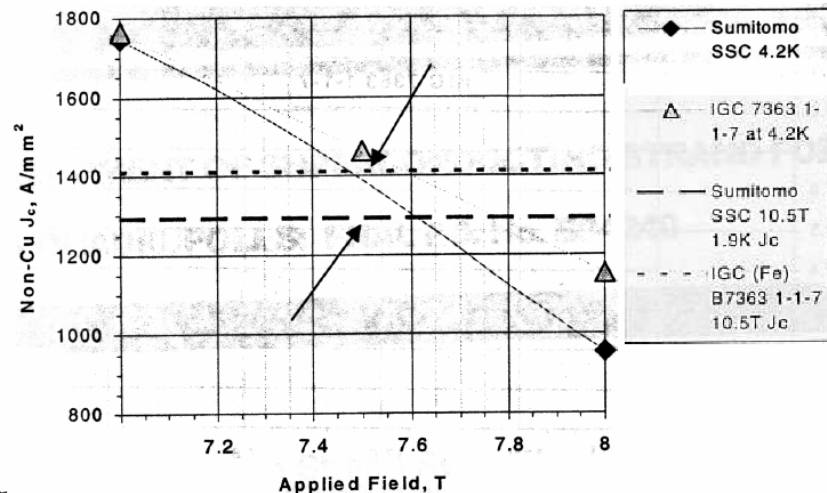


**Table 5 Comparison of critical current densities for SSC Sumitomo strand and OI-ST strands**

Field	Sumitomo SSC 4.2K	OI-ST 4123 1A6 at 4.2K
5	2767	3071
7	1748	1770
7.5		1466
8	956	1183
5T/7T	1.58	1.74
5T/8T	2.89	2.60

